Synthesis of (^{t}Bu$_3$SiNH)$_2$ClW≡WCl(NHSi^{t}Bu$_3$)$_2$ and Its Degradation via NH Bond Activation

Stephen M. Holmes, Daniel F. Schafer II, Peter T. Wolczanski,* and Emil B. Lobkovsky

Contribution from the Department of Chemistry & Chemical Biology, Baker Laboratory, Cornell University, Ithaca, New York 14853

Received April 13, 2001

Abstract: Treatment of $NaW_2Cl_7(THF)_5$ with 4 equiv of ^{t}Bu$_3$SiNHLi afforded the C_2 W(III) dimer [(^{t}Bu$_3$SiNH)$_2$WCl]$_2$ (**1**, d(W≡W) = 2.337(2) Å), which is a rare, primary amide $M_2X_4Y_2$ species. Its degradation provided evidence of NH bond activation by the ditungsten bond. Addition of 2 equiv of ^{t}Bu$_3$SiNHLi or TlOSi^{t}Bu$_3$ to **1** yielded H_2 and hydride (^{t}Bu$_3$SiN)$_2$(^{t}Bu$_3$SiNH)WH (**2**, d(WH) = 1.67(3) Å) or (^{t}Bu$_3$SiN)$_2$-(^{t}Bu$_3$SiO)WH (**3**). Thermolysis (60 °C, 16 h) of **1** in py gave (^{t}Bu$_3$SiN)$_2$WHCl(py) (**4**-py, 40−50%), (^{t}Bu$_3$-SiN)$_2$WCl$_2$(py) (**6**-py, 10%), and (^{t}Bu$_3$SiN)$_2$HW(μ-Cl)(μ-H)$_2$W(NSi^{t}Bu$_3$)py$_2$ (**5**-py$_2$, 5%), whereas thermolysis in DME produced (^{t}Bu$_3$SiN)$_2$WCl(OMe) (**7**, 30%), (^{t}Bu$_3$SiN)$_2$WCl$_2$ (**6**, 20%), and (^{t}Bu$_3$SiN)$_2$HW(μ-Cl)(μ-H)$_2$W(NSi^{t}Bu$_3$)DME (**5**-DME, 3%). Compound **7** was independently produced via thermolysis of **4**-py and DME (−MeOEt, −py), and THF and ethylene oxide addition to hydride **2** gave (^{t}Bu$_3$SiN)$_2$(^{t}Bu$_3$SiNH)WO^{n}Bu (**8**) and (^{t}Bu$_3$SiN)$_2$(^{t}Bu$_3$SiNH)WOEt (**9**), respectively. Dichloride **6** was isolated from $SnCl_4$ treatment of **1** with the loss of H_2. Sequential NH bond activations by the W_2 core lead to "(^{t}Bu$_3$SiN)$_2$WHCl" (**4**) and subsequent thermal degradation products. Thermolysis of **1** in the presence of H$_2$C=CH^{t}Bu and PhC≡CPh trapped **4** and generated (^{t}Bu$_3$SiN)$_2$W(^{neo}Hex)Cl (**10**) and a ∼6:1 mixture of (^{t}Bu$_3$SiN)$_2$WCl(*cis*-CPh=CPhH) (**11**-*cis*) and (^{t}Bu$_3$SiN)$_2$WCl(*trans*-CPh=CPhH) (**11**-*trans*), respectively. Thermolysis of the latter mixture afforded (^{t}Bu$_3$SiNH)(^{t}Bu$_3$SiN)WCl(η^2-PhCCPh) (**12**) as the major constituent. Alkylation of **1** with MeMgBr produced (^{t}Bu$_3$SiN)$_2$W(CH$_3$)$_2$ (**13**), as did addition of 2 equiv of MeMgBr to **6**. X-ray crystal structure determinations of **1**, **2**, **5**-py$_2$, **6**-py, **11**-*trans*, and **12** confirmed spectroscopic identifications. A general mechanism that features a sequence of NH activations to generate **4**, followed by chloride metathesis, olefin insertion, etc., explains the formation of all products.

Introduction

In displaying the reactivity of multiple bonds,[1] triply bonded dinuclear species, especially group 6 $X_nY_{3-n}M{\equiv}MX_nY_{3-n}$ (n = 2, 3; X, Y = R, OR, ERR′ (E = N, P, As), SR, SiR$_3$, etc.) complexes,[2] have played a crucial role by exhibiting a broad spectrum of transformations involving ligands and various substrates. While diverse in terms of ligand type, primary amide ligation is uncommon to this particular class of molecules. Examples typically contain additional donors that reduce the coordinative unsaturation intrinsic to the $[X_nY_{3-n}M]_2$ (n = 2,3) type dimers, including amines that hydrogen bond with other ligands.[3−5] In contrast to common triply bonded dinuclear compounds containing secondary amides,[1,2] the proximity of the reactive NH functionality of $X_nM{\equiv}M(NHR)Y_m$ (n = 3, m = 2) to the coordinatively unsaturated metal centers comprising the triple bond may render such a ligand susceptible to degradation.

During the course of optimizing the synthesis of (^{t}Bu$_3$SiN)$_2$-(^{t}Bu$_3$SiNH)WH (**2**)[6] from $NaW_2Cl_7(THF)_5$[7,8] and (^{t}Bu$_3$SiNH)-Li,[9,10] NMR spectroscopic studies hinted at the retention of the W_2 unit during early stages of the reaction. Given the steric features of the tri-*tert*-butylsilamide ligand, it seemed likely that tungsten−tungsten triply bonded intermediates might prove isolable, providing a means to independently monitor the degradation of a primary amide in the presence of a multiple bond. Reported herein is the synthesis and isolation of (^{t}Bu$_3$-SiNH)$_2$ClW≡WCl(NHSi^{t}Bu$_3$)$_2$ (**1**) and studies of its derivatization and decomposition.[11]

Results

(^{t}Bu$_3$SiNH)$_2$ClW≡WCl(NHSi^{t}Bu$_3$)$_2$ (1). 1. Synthesis. A benzene solution of $NaW_2Cl_7(THF)_5$[7,8] and 4 equiv of ^{t}Bu$_3$-

(1) Cotton, F. A.; Walton, R. A. *Multiple Bonds Between Metal Atoms*; Oxford University Press: New York, 1993.

(2) (a) Chisholm, M. H. *Acc. Chem. Res.* **1990**, *23*, 419−425. (b) Chisholm, M. H. *J. Organomet. Chem.* **1990**, *400*, 235−253. (c) Chisholm, M. H. *Pure Appl. Chem.* **1991**, *63*, 665−680. (d) Chisholm, M. H.; Kramer, K. S.; Martin, J. D.; Huffman, J. C.; Lobkovsky, E. B.; Streib, W. E. *Inorg. Chem.* **1992**, *31*, 4469−4474. (e) Cayton, R. H.; Chacon, S. T.; Chisholm, M. H.; Folting, K.; Moodley, K. G. *Organometallics* **1996**, *15*, 992−997.

(3) (a) Bradley, D. C.; Errington, R. J.; Hursthouse, M. B.; Short, R. L. *J. Chem. Soc., Dalton Trans.* **1986**, 1305−1307. (b) Bradley, D. C.; Hursthouse, D. C.; Powell, H. R.; *J. Chem. Soc., Dalton Trans.* **1989**, 1537−1541.

(4) Abbott, R. G.; Cotton, F. A.; Falvello, L. R. *Inorg. Chem.* **1990**, *29*, 514−521.

(5) (a) Chisholm, M. H.; Parkin, I. P.; Streib, W. E.; Folting, K. S. *Polyhedron* **1991**, *10*, 2309−2316. (b) Baxter, D. V.; Chisholm, M. H.; Gama, G. J.; DiStasi, V. F. *Chem. Mater.* **1996**, *8*, 1222−1228.

(6) Schafer, D. F., II; Wolczanski, P. T. *J. Am. Chem. Soc.* **1998**, *120*, 4881−4882.

(7) Chisholm, M. H.; Eichorn, B. W.; Folting, K.; Huffman, J. C.; Ontiveros, C. D.; Streib, W. E.; Van Der Sluys, W. G. *Inorg. Chem.* **1987**, *26*, 3182−3186.

(8) Schrock, R. R.; Sturgeoff, L. G.; Sharp, P. R. *Inorg. Chem.* **1983**, *22*, 2801−2806.

(9) Nowakowski, P. M.; Sommer, L. H. *J. Organomet. Chem.* **1979**, *178*, 95−103.

(10) Cummins, C. C.; Van Duyne, G. D.; Schaller, C. P.; Wolczanski, P. T. *Organometallics* **1991**, *10*, 164−170.

(11) Schafer, D. F., II. Ph.D. Thesis, Cornell University, Ithaca, NY, 1999.

10.1021/ja010957h CCC: $20.00
Published on Web 10/09/2001

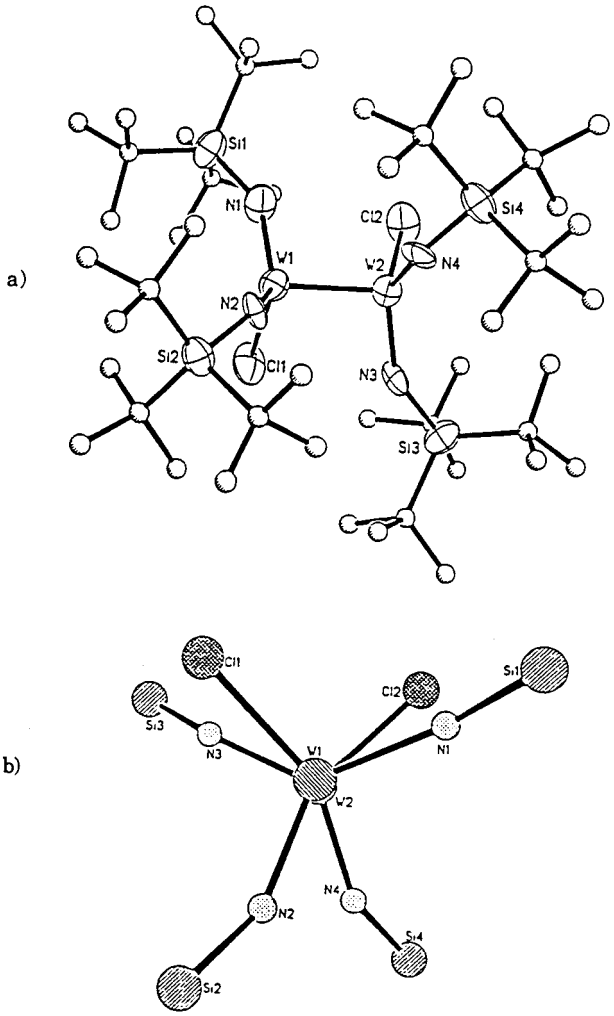

Figure 1. (a) Molecular structure of $(^tBu_3SiNH)_2ClW{\equiv}WCl(NHSi^tBu_3)_2$ (**1**); view down the C_2 axis. (b) View of the core down the W≡W bond.

SiNHLi[9,10] turned from emerald green to brown over the course of 1 h, producing the dark red W(III) dimer $[(^tBu_3SiNH)_2WCl]_2$ (**1**) which was isolated in 48% yield from hexane (eq 1). The infrared spectrum of **1** exhibited an absorption in the NH stretching region ($\nu_{NH} = 3164\ cm^{-1}$) and ^1H and $^{13}C\{^1H\}$ NMR spectra (Table 1) that revealed two distinct amide ligands indicative of the predicted C_2 symmetry.[12] When stored at −20 °C, **1** is a stable crystalline solid, but it is also conveniently generated in situ for preparative applications.

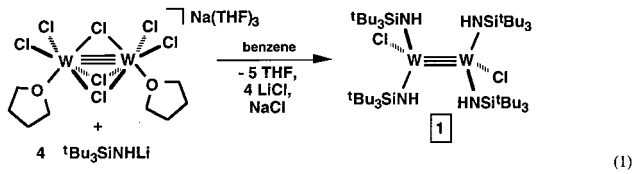

(1)

2. Structure. The single-crystal X-ray structure determination (Table 2) of $(^tBu_3SiNH)_2ClW{\equiv}WCl(NHSi^tBu_3)_2$ (**1**) confirmed its C_2 symmetry. After exhaustive crystallization attempts, only a moderate quality data set could be obtained for **1**, requiring isotropic refinement of its carbons, but the seminal features of the molecule are apparent as Figure 1a illustrates. A slightly elongated W≡W (2.337(2) Å) bond[15] and normal W−Cl bond lengths $(2.309(8)_{av}$ Å) were observed for **1**,[1,2] as compared with the respective 2.285(2) and 2.329(6) Å distances in $[(Me_2N)_2WCl]_2$ (Table 3).[13] Because of the extreme bulk of the $^tBu_3SiNH$ ligands, the molecular geometry about the ditungsten core of **1** contrasts greatly from that of C_{2h} (anti) $[(Me_2N)_2W(Cl)]_2$, as the view down the W_2 vector in Figure 1b shows. A distorted disposition of the ligand set (dihedral ∠Cl1−W1−W2−Cl2 = 89.4°) is observed, where chlorides and amides on adjacent tungstens approach an eclipsing conformation (dihedral ∠N1−W1−W2−Cl2 = 21.2°, dihedral ∠N3−W2−W1−Cl1 = 21.9°), while the remaining amides skew away from one another (dihedral ∠N2−W1−W2−N4 = 38.3°). The set of four amides (∠N1−W1−N2 = 129.3 (9)°, ∠N3−W2−N4 = 126.8(8)°) distort toward a D_{2d} arrangement, as had been predicted for $[(^tBu_3SiO)_2WCl]_2$.[12] Relatively long tungsten−nitrogen amide bond lengths ranging from 1.97(2) to 1.99(2) Å are observed, while the W−N−Si angles (146(1)° to 150(1)°) are smaller than those of trisamido,[10] bisamidoimido,[14] and bisimidoamido cores,[11] perhaps reflecting a greater steric influence from the adjacent tungsten rather than from the accompanying amide.

$(^tBu_3SiN)_2(^tBu_3SiZ)WH$ (Z = NH, 2; Z = O, 3). 1. Synthesis. Treatment of $NaW_2Cl_7(THF)_5$[7,8] with 6 equiv of $^tBu_3SiNHLi$[9,10] in benzene for 1 h at 23 °C, followed by 4 h at 100 °C, generated dihydrogen (0.78 equiv by Toepler pump) and the four-coordinate bisimide amide hydride $(^tBu_3SiN)_2(^tBu_3SiNH)WH$ (**2**)[6] in 50−60% yield after hexane filtration and recrystallization from THF (eq 2). $[(^tBu_3SiNH)_2WCl]_2$ (**1**) was shown by ^1H NMR spectroscopy to be a competent intermediate in the reaction, and treatment of it with 2 equiv of $^tBu_3SiNHLi$ in C_6D_6 effected its conversion to **2** (eq 3). Each dimer undergoes a 6 e^- oxidation in forming 2 equiv of the W(VI) product as two protons are converted to terminal hydrides, representing a formal 4 e^- reduction, and two combine to form H_2.

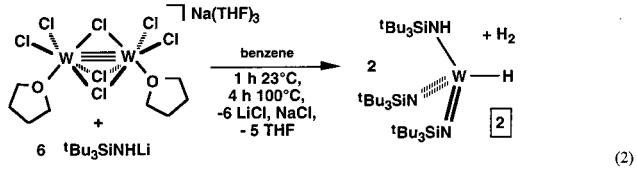

(2)

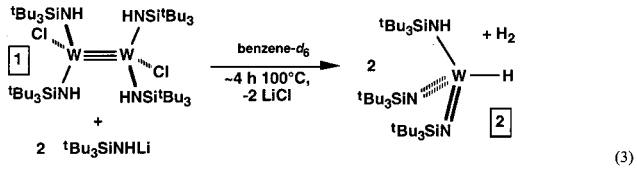

(3)

Colorless hydride $(^tBu_3SiN)_2(^tBu_3SiNH)WH$ (**2**) may be heated in benzene at 200 °C for > 1 month without noticeable decomposition. Compound **2** exhibits C_s symmetry according to its ^1H and $^{13}C\{^1H\}$ NMR spectra, and the hydride resonance is located as δ 13.34 with $^1J_{WH} = 356$ Hz, consistent with a WH bond of significant s-character typical of a low coordinate "hydridic" species accompanied by hard ancillary ligands.[15] Its 14% integrated satellite intensity confirms the assignment as a

(12) Miller, R. L.; Lawler, K. A.; Bennett, J. L.; Wolczanski, P. T. *Inorg. Chem.* **1996**, *35*, 3242−3253.

(13) Akiyama, M.; Chisholm, M. H.; Cotton, F. A.; Extine, M. W.; Murillo, C. A. *Inorg. Chem.* **1977**, *16*, 2407−2411.

(14) Schaller, C. P.; Cummins, C. C.; Wolczanski, P. T. *J. Am. Chem. Soc.* **1996**, *118*, 591−611.

(15) (a) Vanderzeijden, A. A. H.; Sontag, C.; Bosch, H. W.; Shklover, V.; Berke, H.; Nanz, D. Vonphilipsborn, W. *Helv. Chim. Acta* **1991**, *74*, 1194−1204. (b) Templeton, J. L.; Philipp, C. C.; Pregosin, P. S.; Ruegger, H. *Magn. Reson. Chem.* **1993**, *31*, 58−62.

Table 1. ^{1}H and ^{13}C{^{1}H} NMR Spectral Data (δ, Assignment, Multiplicity, J (Hz)) for [(^{t}Bu$_3$SiNH)$_2$WCl]$_2$ (**1**) and Derivatives in C_6D_6 unless Otherwise Noted

	^{1}H NMR δ, multiplicity, assignment, J (Hz)			^{13}C{^{1}H} NMR δ, assignment, J (Hz)		
compound	((H$_3$C)$_3$C)$_3$	NH	R/H	C(*C*H$_3$)$_3$	*C*(CH$_3$)$_3$	R
[(^{t}Bu$_3$SiNH)$_2$WCl]$_2$ (**1**)	1.25	7.60		31.34	24.08	
	1.26	10.12		31.46	24.13	
(^{t}Bu$_3$SiN)$_2$(^{t}Bu$_3$SiNH)WH (**2**)	1.18[a]	7.41	13.34, J_{WH} = 356	30.53	22.72[b]	
	1.34[a]			31.11	23.95[b]	
(^{t}Bu$_3$SiN)$_2$(^{t}Bu$_3$SiO)WH (**3**)	1.18[a]		13.36, J_{WH} = 391	30.09	23.00[b]	
	1.33[a]			31.04	23.80[b]	
(^{t}Bu$_3$SiN)$_2$WClH(py) (**4**-py)	1.42		6.32, t, *m*-CH, 6.4	30.79	24.55	124.88, *p*-C
			6.58, t, *p*-CH, 7.4			139.15, *m*-C
			8.92, d, *o*-CH, 4.8			152.13, *o*-C
			15.96, J_{WH} = 217			
(^{t}Bu$_3$SiN)$_2$HW(μ-Cl)(μ-H)$_2$	1.30[a]		6.36, t, *m*-CH, 7.6	31.04	23.49	124.34, *p*-C
W(NSi^{t}Bu$_3$)py$_2$ (**5**-py$_2$)	1.58[a]		6.52, t, *p*-CH, 7.6	31.40	24.33	137.80, *m*-C
			8.62, d, *o*-CH, 4.8			154.32, *o*-C
			7.79, d, μ-H, 4.8, J_{WH} = 139, 20			
			15.79, t, H, 4.8, J_{WH} = 237			
(^{t}Bu$_3$SiN)$_2$HW(μ-Cl)(μ-H)$_2$	1.27[a]		2.27, m, C*H*HO			
W(NSi^{t}Bu$_3$)DME (**5**-DME)	1.58[a]		2.29, m, CH*H*O			
			3.80, OCH$_3$			
			5.17, d, μ-H, 4, J_{WH} = 173, 17			
			14.90, t, H, 4, J_{WH} = 245			
(^{t}Bu$_3$SiN)$_2$WCl$_2$ (**6**)	1.27			30.51	25.19	
(^{t}Bu$_3$SiN)$_2$WCl$_2$py (**6**-py)	1.35		6.38, *m*-CH[c]	31.32	26.32	*c*
			6.59, *p*-CH[c]			
			8.89, *o*-CH[c]			
(^{t}Bu$_3$SiN)$_2$W(OMe)Cl (**7**)	1.30		4.19, OCH$_3$			
	1.20[d]		4.68, OCH$_3$[d]	31.12[d]	24.50[d]	30.57, OCH$_3$[d]
(^{t}Bu$_3$SiN)$_2$(^{t}Bu$_3$SiNH)WO^{n}Bu (**8**)	1.27[a]	5.12	0.85, t, CH$_3$, 7	31.01	23.69[b]	13.91, CH$_3$
	1.37[a]		1.37, m, CH$_2$	31.36	24.49[b]	19.04, CH$_2$
			1.58, m, CH$_2$			35.74, CH$_2$
			4.63, t, OCH$_2$, 6			79.66, OCH$_2$
(^{t}Bu$_3$SiN)$_2$(^{t}Bu$_3$SiNH)WOEt (**9**)	1.26[a]	5.09	1.17, t, CH$_3$, 7	31.00	23.69[b]	19.14, CH$_3$
	1.35[a]		4.59, q, OCH$_2$, 7	31.35	24.49[b]	75.46, OCH$_2$
(^{t}Bu$_3$SiN)$_2$ClW(CH$_2$CH$_2$^{t}Bu) (**10**)	1.30		0.87, s, ^{t}Bu	29.53	24.78	23.01, C(CH$_3$)$_3$
			2.08, m, CH$_2$			29.12, C(CH$_3$)$_3$
			2.65, m, CH$_2$			46.72, C$_\beta$H$_2$
						56.94, C$_\alpha$H$_2$, J_{WC} = 95
(^{t}Bu$_3$SiN)$_2$WCl	1.32		6.88, m, Ph, 7	30.75	24.80	128.75, *o*-C$_\beta$
(*cis*-CPh=CPhH) (**11**-*cis*)[e,f]			7.01, m, Ph, 8.8			129.65, *p*-C$_\beta$
			7.13, m, Ph, 8.2			129.68, *o*-C$_\alpha$
			7.39, d, *o*-CH, 7.2			130.06, *m*-C$_\beta$
			7.92, s, β-CH, J_{WH} = 7.6			130.38, *m*-C$_\alpha$
						131.92, *p*-C$_\alpha$
						136.09, *ipso*-C$_\beta$
						137.46, *ipso*-C$_\alpha$
						139.79, β-CHPh
						192.57, α-CPh,
						J_{WC} = 153
(^{t}Bu$_3$SiN)$_2$WCl	1.31		7.13, m, Ph, 7.6	31.27	25.47	129.75, *o*-C$_\beta$
(*trans*-CPh=CPhH) (**11**-*trans*)[e,f]			7.26, m, Ph, 7.6			131.25, *o*-C$_\alpha$
			7.65, d, *o*-CH, 7.2			133.15, *p*-C$_\beta$
			7.83, d, *o*-CH, 7.2			133.43, *m*-C$_\beta$
			8.38, s, β-CH, J_{WH} = 8.4			133.97, *p*-C$_\alpha$
						134.69, *m*-C$_\alpha$
						136.67, *ipso*-C$_\beta$
						138.67, *ipso*-C$_\alpha$
						144.69, β-CHPh
						190.59, α-CPh,
						J_{WC} = 146
(^{t}Bu$_3$SiNH)(^{t}Bu$_3$SiN)WCl	1.06[g]	8.08	7.08, m, Ph	30.15	23.46[g]	128.42, 129.40, *p*-C
(η^2-PhCCPh) (**12**)[e]	1.22[g]		7.23, t, *p*-CH, 7.6	30.40	24.81[g]	128.58, *m/o*-C
			7.33, t, *p*-CH, 7.6			128.70, *m/o*-C
			7.98, d, *o*-CH, 7.6			129.70, *m/o*-C
			8.00, d, *o*-CH, 7.6			132.23, *m/o*-C
						138.15, 140.47, C$_{ipso}$
						175.08, CPh
						189.80, CPh
(^{t}Bu$_3$SiN)$_2$W(CH$_3$)$_2$ (**13**)	1.29		1.17, s, Me, J_{WH} = 8.8	30.71	24.43	48.44, Me, J_{WC} = 107

[a] First resonance 27H; second, 54H. [b] First resonance amide/siloxide; second, imide. [c] Resonances broad because of exchange with free py; py resonances not located in the ^{13}C{^{1}H} NMR spectrum, presumably because of exchange broadening. [d] THF-d_8. [e] ^{13}C{^{1}H} phenyl ring assignments tentative. [f] C$_\alpha$ and C$_\beta$ refer to α and β phenyl ring carbons, whereas α-C and β-C refer to the α and β carbons of the alkene. [g] Assignments nebulous.

Table 2. Crystallographic Data for [(^{t}Bu$_3$SiNH)$_2$WCl]$_2$ (**1**), (^{t}Bu$_3$SiN)$_2$(^{t}Bu$_3$SiNH)WH (**2**), (^{t}Bu$_3$SiN)$_2$HW(μ-Cl)(μ-H)$_2$W(NSi^{t}Bu$_3$)py$_2$ (**5**-py$_2$), (^{t}Bu$_3$SiN)$_2$WCl$_2$(py) (**6**-py), (^{t}Bu$_3$SiN)$_2$WCl(*trans*-CPh=CPhH) (**11**-*trans*), and (^{t}Bu$_3$SiNH)(^{t}Bu$_3$SiN)WCl(PhCCPh) (**12**)

	1	**2**	**5**-py$_2$	**6**-py[a]	**11**-*trans*	**12**
formula	$C_{54}H_{124}N_4Si_4Cl_2W_2$	$C_{36}H_{83}N_3Si_3W$	$C_{46}H_{94}N_5Si_3ClW_2$	$C_{29}H_{59}N_3Si_2Cl_2W$	$C_{38}H_{65}N_2Si_2ClW$	$C_{38}H_{65}N_2S_2ClW$
formula wt	1380.53	826.18	1204.69	760.73	825.42	825.42
space group	$P2_1/n$	$P2_1/n$	$P2_1/n$	$C2/c$	$P2_1/c$	$P2_1/c$
Z	4	4	4	8	4	4
a, Å	13.7997(4)	13.4342(2)	13.7991(11)	11.999(2)	12.081(2)	14.393(2)
b, Å	23.8392(2)	16.2068(1)	24.343(2)	12.801(3)	12.080(2)	17.903(3)
c, Å	21.7517(3)	20.8307(3)				
α, deg	90	90	90	90	90	90
β, deg	100.117(2)	90.477(1)	92.598(2)	93.97(3)	101.20(3)	110.903(3)
γ, deg	90	90	90	90	90	90
V, Å^3	7044.5(3)	4535.2(1)	5618.0(8)	3550.4(12)	4163.1(14)	4105.8(10)
ρ_{calc}, g·cm^{-3}	1.302	1.209	1.423	1.423	1.341	1.335
μ, cm^{-1}	3.439	2.651	4.236	3.493	2.925	2.963
temp, K	293(2)	293(2)	173(2)	173(2)	173(2)	173(2)
λ, Å	0.710 73	0.710 73	0.710 73	0.710 73	0.943 00	0.710 73
R indices, $[I > 2\sigma(I)]$[b,c]	$R_1 = 0.0970$, $wR_2 = 0.2486$	$R_1 = 0.0319$, $wR_2 = 0.0789$	$R_1 = 0.0451$, $wR_2 = 0.0729$	$R_1 = 0.0418$, $wR_2 = 0.0956$	$R_1 = 0.0626$, $wR_2 = 0.1846$	$R_1 = 0.0432$, $wR_2 = 0.0856$
R indices (all data)[b,c]	$R_1 = 0.1726$, $wR_2 = 0.3030$	$R_1 = 0.0493$, $wR_2 = 0.0943$	$R_1 = 0.1253$, $wR_2 = 0.1079$	$R_1 = 0.0793$, $wR_2 = 0.1203$	$R_1 = 0.0660$, $wR_2 = 0.1890$	$R_1 = 0.0656$, $wR_2 = 0.0927$
GOF[d]	1.010	1.088	0.993	0.984	1.151	0.988

[a] The asymmetric unit is half of the formula unit. [b] $R_1 = \sum||F_o| - |F_c||/\sum|F_o|$. [c] $wR_2 = [\sum w(|F_o| - |F_c|)^2/\sum \omega F_o^2]^{1/2}$. [d] GOF (all data) $= [\sum w(|F_o| - |F_c|)^2/(n-p)]^{1/2}$; n = number of independent reflections, p = number of parameters.

Table 3. Selected Interatomic Distances (Å) and Angles (deg) for [(^{t}Bu$_3$SiNH)$_2$WCl]$_2$ (**1**)

				Interatomic Distance			
W1−W2	2.337(2)	W1−N1	1.98(2)	W2−N3	1.97(2)	W1−Cl1	2.310(8)
N−Si$_{av}$	1.78(2)	W1−N2	1.97(2)	W2−N4	1.99(2)	W2−Cl2	2.308(7)
				Angle			
W1−N1−Si1	149.5(15)	W2−W1−Cl1	100.3(2)	W1−W2−N3	99.4(6)	N3−W2−Cl2	108.8(6)
W1−N2−Si2	146.3(12)	W1−W2−Cl2	100.8(2)	W1−W2−N4	103.6(6)	N4−W2−Cl2	112.9(6)
W2−N3−Si3	149.1(12)	W2−W1−N1	100.3(7)	N1−W1−Cl1	108.0(7)	N1−W1−N2	129.3(9)
W2−N4−Si4	148.0(12)	W1−W2−N2	101.8(6)	N2−W1−Cl1	112.1(7)	N3−W2−N4	126.8(8)

Table 4. Selected Interatomic Distances (Å) and Angles (deg) for (^{t}Bu$_3$SiN)$_2$(^{t}Bu$_3$SiNH)WH (**2**)[a]

				Interatomic Distance			
W−H	1.67(3)	W−N1	1.812(3)	W−N2	1.827(2)	W−N3	1.832(3)
N1−Si1	1.761(3)	N2−Si2	1.756(3)	N3−Si3	1.748(3)		
				Angle			
W−N1−Si1	164.9(2)		N1−W−N2	116.84(12)		H−W−N1	100.0(8)
W−N2−Si2	162.0(2)		N1−W−N3	115.17(13)		H−W−N2	99.7(8)
W−N3−Si3	162.4(2)		N2−W−N3	115.46(13)		H−W−N3	106.2(8)

[a] Imide and amide ligands statistically disordered.

terminal hydride, and the infrared spectrum of **2** exhibits characteristic W−H (ν_{WH} = 1910 cm^{-1})[16] and N−H (ν_{NH} = 3234 cm^{-1}) stretching absorptions. Similar spectral properties are observed for (^{t}Bu$_3$SiN)$_2$(^{t}Bu$_3$SiO)WH (**3**), which was prepared from **1** generated in situ and 2 equiv of TlOSi^{t}Bu$_3$ in THF according to eq 4. The hydride of C_s **3** resonated at δ

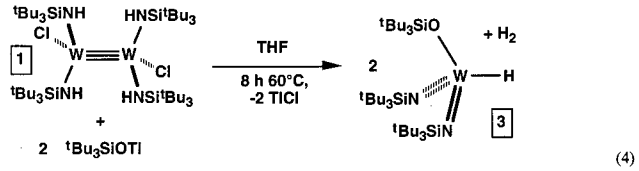

(4)

13.36 ($^1J_{WH}$ = 391 Hz, 14%) in its ^{1}H NMR spectrum, and an IR stretch of 1941 cm^{-1} was assigned to it.

Addition of anionic ligands ^{t}BuSiZ$^-$ (Z = NH, O) to **1** either promotes degradation of the ditungsten unit or traps intermediates generated upon thermal decomposition. For example, it is convenient to think of the W(III) being oxidized to W(VI) upon heating to provide "(^{t}Bu$_3$SiN)$_2$WHCl" (**4**), which can then be scavenged accordingly by the aforementioned anions or substrates that react with hydride.

2. Structure of (^{t}Bu$_3$SiN)$_2$(^{t}Bu$_3$SiNH)WH (2). A single-crystal X-ray structural examination (Table 2, Table 4) of (^{t}Bu$_3$SiN)$_2$(^{t}Bu$_3$SiNH)WH (**2**) confirmed its monomeric nature in the solid state, as Figure 2 reveals. The hydride was located, and its bond length of 1.67(3) Å is reasonable when compared with the sum of W and H covalent radii (1.62 Å).[17] There is a moderate distortion from tetrahedral resulting from intraligand steric effects, as the N−W−N angles of 115.8(9)° (av) are significantly greater than the H−W−N angles (102.0(36)° (av)). The imides and amide adopt a pinwheel arrangement about the W ($\angle$W−N−Si = 163.1 (16)° (av)) similar to those of (^{t}Bu$_3$SiNH)$_3$ZrMe[10] and (^{t}Bu$_3$SiNH)$_2$(^{t}Bu$_3$SiN)ZrTHF,[14] but all the W−N bond lengths are similar (1.824(10)° (av)) and presumably reflect a statistical disorder of the imides and amide. If the tungsten−amide distance is estimated to be 1.91 Å, a value

(16) For a recent discussion of tungsten−hydride IR spectral features, see: Hascall, T.; Rabinovich, D.; Murphy, V. J.; Beachy, M. D.; Friesner, R. A.; Parkin, G. *J. Am. Chem. Soc.* **1999**, *121*, 11402−11417.

(17) For a recent discussion of the covalent radius of tungsten, see: Murphy, V. J.; Rabinovich, D.; Hascall, T.; Kloowster, W. T.; Koetzle, T. F.; Parkin, G. *J. Am. Chem. Soc.* **1998**, *120*, 4372−4387.

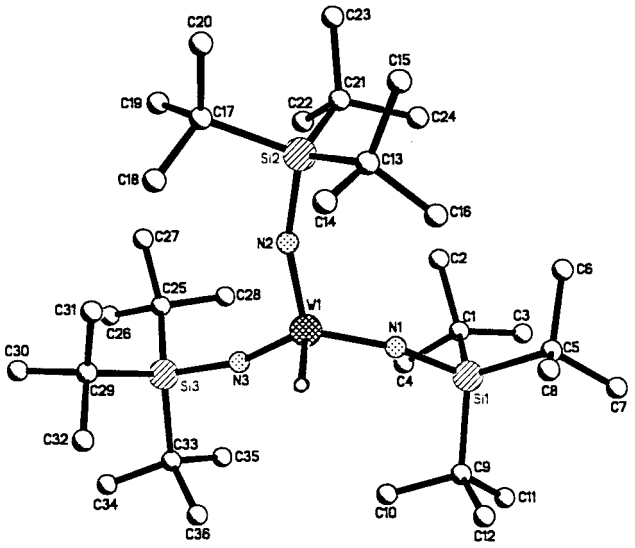

Figure 2. Molecular structure of (^{t}Bu$_3$SiN)$_2$(^{t}Bu$_3$SiNH)WH (**2**).

reasonable for this bulky ligand (vide infra), and a mean tunsten−imide distance of 1.72 Å is used,[18] their weighted average bond length is 1.85 Å, a value similar to the *d*(WN) obtained for **2**.

Thermolyses of (^{t}Bu$_3$SiNH)$_2$ClW≡WCl(NHSi^{t}Bu$_3$)$_2$ (1). 1. Pyridine. Thermolysis (85°, 24 h) of (^{t}Bu$_3$SiNH)$_2$ClW≡WCl(NHSi^{t}Bu$_3$)$_2$ (**1**) in benzene afforded copious amounts of ^{t}Bu$_3$SiNH$_2$ and ^{t}Bu$_3$SiNH$_3^+$ according to ^{1}H NMR spectroscopy, but little tungsten-containing material remained soluble, and no further characterizations were attempted. Reasoning that the putative degradation product "(^{t}Bu$_3$SiN)$_2$WHCl" (**4**) was unstable with respect to aggregation and amine loss, etc., the thermolyses were undertaken in solvents with some donor capacity.

Scheme 1 provides the results of the thermal degradation (60 °C, 16 h) of [(^{t}Bu$_3$SiNH)$_2$WCl]$_2$ (**1**) in pyridine, as determined from mass balance and a subsequent ^{1}H NMR (benzene-d_6) assay of the rough product distribution. Use of more polar solvents for the ^{1}H NMR assay (e.g., THF-d_8) afforded little additional information, and fractional crystallizations from polar media were ineffective because of high solubilities. Chromatographic efforts also proved impractical; hence, separation was achieved via fractional crystallizations, primarily from pentane, thereby permitting characterization.

As shown, aside from the 5−10% of ^{t}Bu$_3$SiNH$_2$ and ^{t}Bu$_3$SiNH$_3^+$ (presumably as the choride salt) observed, the dominant tungsten-containing product is (^{t}Bu$_3$SiN)$_2$WHCl(py) (**4**-py), which was isolated in 28% yield (based on W) as colorless crystals from pentane. An infrared band at 1874 cm^{-1} is assigned to the hydride, which was also observed as a singlet with satellites (J_{WH} = 217 Hz) at δ 15.96 in the ^{1}H NMR spectrum in addition to ^{t}Bu and pyridine resonances. A pseudo-tbp (trigonal bipyramidal) structure[19] with equatorial imides and hydride is drawn for **4**-py, thereby averting a 90° py/Cl interaction, but this cannot be distinguished from an axial hydride structure on a spectroscopic basis. The hydride and alkyl group of pseudo-tbp (^{t}Bu$_3$SiO)$_3$HTaCH$_2$CH$_2$O^{t}Bu[20] are found in equatorial sites that favor more covalently bound ligands. In contrast, the imides of pseudo-tbp (^{t}Bu$_3$SiN)$_2$TaMe(py)$_2$[21] are equatorial, but the pyridines occupy both axial and equatorial sites, and the Me is unexpectedly axial.[22] Note that the J_{WH} is consistent with the diminished amount of s-character[15] of a 5-coordinate complex relative to (^{t}Bu$_3$SiN)$_2$(^{t}Bu$_3$SiNH)WH (**2**) and (^{t}Bu$_3$SiN)$_2$(^{t}Bu$_3$SiO)WH (**3**). Other 5-coordinate complexes of the type {Li(^{t}Bu$_3$SiN)$_2$(^{t}Bu$_3$SiNH)}WH$_{ax}$(R$_{ax}$)[11] possess J_{WH} values that are lower, yet in a similar range (152−171 Hz when R is sp^3) when R and H oppose one another in the basal plane of a distorted square pyramid.

Another hydride product, (^{t}Bu$_3$SiN)$_2$HW(μ-Cl)(μ-H)$_2$W(NSi-^{t}Bu$_3$)py$_2$ (**5**-py$_2$) was obtained in 7% isolated yield (based on **1**; 3% based on W) as purple crystals from pentane. Two distinct types of imido ligands are observed in a 2:1 ratio in the ^{13}C-{^{1}H} and ^{1}H NMR spectra of **5**-py$_2$, along with two equivalent pyridines and two types of hydrides. A lone terminal hydride observed as a triplet at δ 15.79 with J_{WH} = 237 Hz is coupled (J = 4.8 Hz) to two equivalent bridging hydrides (δ 7.79, d) that possess two sets of satellite resonances (J_{WH} = 20, 139 Hz) indicative of disparate tungsten centers.[12,23,24] The infrared spectrum of **5**-py$_2$ reveals a terminal hydride band at 1953 cm^{-1}, and bridging hydride stretching absorptions are tentatively assigned to features at 1858 and 1824 cm^{-1}. The latter features are quite high in frequency and suggest that the bridges in **5**-py$_2$ are quite asymmetric, a possibility corroborated by the magnitude of the J_{WH}'s.

The remaining tungsten-containing compounds in the product distribution consist of the dichloride (^{t}Bu$_3$SiN)$_2$WCl$_2$ (**6**) and its pyridine adduct (^{t}Bu$_3$SiN)$_2$WCl$_2$(py) (**6**-py), which each appear as 5−10% of the mixture. Presumably, when the pyridine solvent is removed, some py is lost from **6**-py, resulting in **6**, because the former is made when pyridine is added to the latter. Neither compound was produced with sufficient purity from thermolysis of **1**, so an alternative synthesis was sought. Treatment of [(^{t}Bu$_3$SiNH)$_2$WCl]$_2$ (**1**) with SnCl$_4$(THF)$_2$ in benzene for 16 h at 60 °C afforded (^{t}Bu$_3$SiN)$_2$WCl$_2$ (**6**) in 50% yield as yellow microcrystals. While initially conceived as a

$$\underset{\mathbf{1}}{[(^t\mathrm{Bu_3SiNH})_2\mathrm{WCl}]_2} + \mathrm{SnCl_4(THF)_2} \xrightarrow[60\ ^\circ\mathrm{C},\ 16\ \mathrm{h}]{\mathrm{THF}} \underset{\mathbf{6}}{(^t\mathrm{Bu_3SiN})_2\mathrm{WCl_2}} + \mathrm{H_2} + \text{“}\mathrm{H_2SnCl_2}\text{”} \quad (5)$$

direct oxidation of **1**, a Toepler pump experiment using 1 equiv of SnCl$_4$ measured only 0.95 equiv of H$_2$ released, and no dimer starting material remained. Stoichiometry and the conditions required suggest that SnCl$_4$ may simply serve as a source of chloride for metathesis with transiently generated "(^{t}Bu$_3$SiN)$_2$WHCl" (**4**). Because **6** was obtained for identification, the reaction was not optimized.

2. Dimethoxyethane (DME). A similar thermolysis of [(^{t}Bu$_3$SiNH)$_2$WCl]$_2$ (**1**) was conducted in DME, and a related product distribution was found as Scheme 1 indicates. The primary product (~30%) was the bisimido derivative, (^{t}Bu$_3$SiN)$_2$WCl(OMe) (**7**), whose NMR spectra are consistent with a methoxide (^{1}H NMR (THF-d_8): δ 4.68 (s); ^{13}C{^{1}H} NMR: δ 30.57). The origin of **7** may lie in the intermediacy of a DME

(18) Nugent, W. A.; Mayer, J. M. *Metal-Ligand Multiple Bonds*; John Wiley & Sons: New York, 1988.

(19) Low coordinate, bisimido derivatives of tungsten are rare and require sterically bulky substituents. See: Williams, D. S.; Schofield, M. H.; Schrock, R. R. *Organometallics* **1993**, *12*, 4560−4571.

(20) Strazisar, S. A.; Wolczanski, P. T. Submitted for publication.

(21) Schaller, C. P.; Wolczanski, P. T. *Inorg. Chem.* **1993**, *32*, 131−144.

(22) The chloride in a diarylimido analogue is equatorial. See: Chao, Y. W.; Wexler, P. A.; Wigley, D. E. *Inorg. Chem.* **1990**, *29*, 4592−4594.

(23) Miller, R. L.; Wolczanski, P. T.; *J. Am. Chem. Soc.* **1993**, *115*, 10422−10423.

(24) (a) Miller, R. L. Ph.D. Thesis, Cornell University, Ithaca, NY, 1994. (b) Miller, R. L.; Wolczanski, P. T. Manuscript in preparation.

Scheme 1

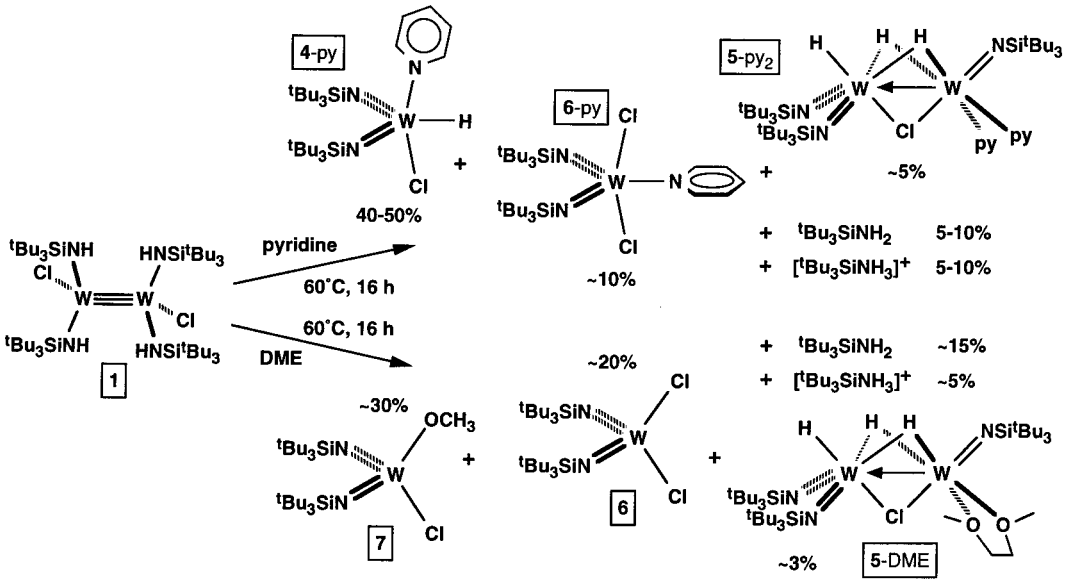

adduct of "(^{t}Bu$_3$SiN)$_2$WHCl" (**4**), such as (^{t}Bu$_3$SiN)$_2$WHCl-(O(Me)CH$_2$CH$_2$OMe) (**4**-DME). Subsequent hydride transfer could provide **7** and EtOMe. Even tungsten hydrides that appear to be electronically satisfied have been shown to attack ethers. For example, thermolysis of (^{t}Bu$_3$SiN)$_2$(^{t}Bu$_3$SiNH)WH (**2**) in THF for 25 h at 145 °C afforded the yellow *n*-butoxide complex, (^{t}Bu$_3$SiN)$_2$(^{t}Bu$_3$SiNH)WO^{n}Bu (**8**, eq 6).

$$(^t\mathrm{Bu_3SiN})_2(^t\mathrm{Bu_3SiNH})\mathrm{WH} \xrightarrow[145\ ^\circ\mathrm{C},\ 25\ \mathrm{h}]{\mathrm{THF}} (^t\mathrm{Bu_3SiN})_2(^t\mathrm{Bu_3SiNH})\mathrm{WO}^n\mathrm{Bu} \quad (6)$$

2 → **8**

$$\mathbf{2} + \mathrm{OCH_2CH_2} \xrightarrow[23\ ^\circ\mathrm{C},\ 5\mathrm{d}]{\text{benzene-}d_6} (^t\mathrm{Bu_3SiN})_2(^t\mathrm{Bu_3SiNH})\mathrm{WOEt} \quad (7)$$

9

Because of its high solubility, **8** was obtained in only 51% yield upon crystallization from Me$_3$SiOSiMe$_3$, but ^{1}H NMR assays of the reaction in THF-d_8 indicated near quantitative conversion. An NMR tube study involving **2** and 5 equiv of ethylene oxide (5 d, 23 °C) revealed an ethoxide group (^{1}H NMR spectroscopy), two imides, and an amide, consistent with the formation of (^{t}Bu$_3$SiN)$_2$(^{t}Bu$_3$SiNH)WOEt (**9**).

Because putative "(^{t}Bu$_3$SiN)$_2$WHCl" (**4**) should be considerably more electrophilic than **2**, it is reasonable to expect that hydride transfer could be effected under thermolysis conditions. A thermolysis of (^{t}Bu$_3$SiN)$_2$WHCl(py) (**4**-py) was conducted in C$_6$D$_6$ with excess DME present in the hope that pyridine loss could be induced to substantiate this point. As eq 8 reveals, (^{t}Bu$_3$SiN)$_2$WCl(OMe) (**7**) is indeed generated upon prolonged heating.

$$(^t\mathrm{Bu_3SiN})_2\mathrm{WHCl(py)} + \mathrm{DME\ (excess)} \xrightarrow[125\ ^\circ\mathrm{C},\ x\ \mathrm{d}]{\text{benzene-}d_6} (^t\mathrm{Bu_3SiN})_2\mathrm{WCl(OMe)} + \mathrm{EtOMe} \quad (8)$$

4-py → **7**

The remaining products are direct analogues to those generated in pyridine. Dichloride (^{t}Bu$_3$SiN)$_2$WCl$_2$ (**6**) was generated in ~20% yield, and a trihydride dinuclear complex, (^{t}Bu$_3$SiN)$_2$HW(μ-Cl)(μ-H)$_2$W(NSi^{t}Bu$_3$)DME (**5**-DME), was identified as a minor product on the basis of the similarity of its ^{1}H NMR spectrum to that of **5**-py$_2$. Its terminal hydride was observed at δ 14.90 (t, J = 4 Hz, J_{WH} = 245 Hz), and the bridging hydrides were assigned to a doublet at δ 5.17 (J = 4 Hz) possessing different satellite couplings (J_{WH} = 173, 17 Hz). **5**-DME was not isolated in sufficient quantity or purity to obtain ^{13}C{^{1}H} NMR spectroscopic studies.

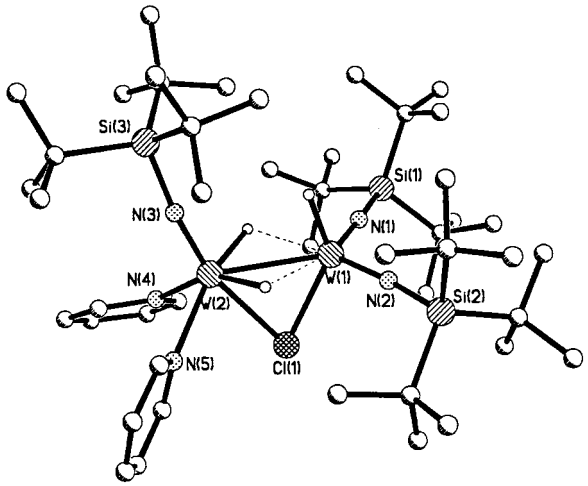

Figure 3. Molecular structure of (^{t}Bu$_3$SiN)$_2$HW(μ-Cl)(μ-H)$_2$W(NSi-^{t}Bu$_3$)py$_2$ (**5**-py$_2$).

3. Structure of (^{t}Bu$_3$SiN)$_2$HW(μ-Cl)(μ-H)$_2$W(NSi^{t}Bu$_3$)py$_2$ (5-py$_2$). A single-crystal X-ray diffractional analysis (Table 2, Table 5) of (^{t}Bu$_3$SiN)$_2$HW(μ-Cl)(μ-H)$_2$W(NSi^{t}Bu$_3$)py$_2$ (**5**-py$_2$) confirmed the structure proposed on the basis of the NMR spectra (Figure 3). The asymmetry of the μ-Cl bridge (d(W−Cl) = 2.456(3), 2.651(2) Å) implies that the structure is best rationalized as a "(^{t}Bu$_3$SiN)py$_2$WH$_2$" fragment trapping the more electrophilic d^0 "(^{t}Bu$_3$SiN)$_2$WHCl" (**4**) piece via formation of a W(IV) → W(VI) donor bond (d(WW) = 2.7878(6) Å). The N1−W1−N2 (112.9(3)°), Cl−W1−N1 (106. (3)°), and Cl−W1−N2 (103.3(2)°) angles of the W(VI) moiety conform to a nearly tetrahedral metal center that must distort enough to accept the (μ-H)$_2$W bridge and metal−metal interaction. All three imides possess normal (d(W(VI)N) = 1.781(7), 1.787(6) Å; d(W(IV)N) = 1.746(7) Å) bond distances,[18] as do the pyridines (d(WN) = 2.227(8), 2.229(7) Å), and the W1−Cl−W2 angle

Table 5. Selected Interatomic Distances (Å) and Angles (deg) for (^{t}Bu$_3$SiN)$_2$HW(μ-Cl)(μ-H)$_2$W(NSi^{t}Bu$_3$)py$_2$ (**5**-py$_2$)[a]

		Interatomic Distance			
W1−W2	2.7878(6)	W1−N1	1.787(6)	W2−N3	1.746(7)
W1−Cl	2.456(3)	W1−N2	1.781(7)	W2−N4	2.227(8)
W2−Cl	2.651(2)	N−Si$_{av}$	1.74(2)	W2−N5	2.229(7)
W2−H1	1.80(9)	W1−H1	2.28(8)		
W2−H2	1.83(8)	W1−H2	2.21(9)		
		Angle			
W1−Cl−W2	66.05(6)	N1−W1−N2	112.9(3)	N1−W1−W2	123.7(2)
Cl−W1−W2	60.34(5)	N1−W1−Cl	106.4(3)	N2−W1−W2	123.3(2)
Cl−W2−W1	53.61(3)	N2−W1−Cl	103.3(2)	N3−W2−W1	110.8(3)
W1−N1−Si1	177.4(5)	N3−W2−N4	107.2(3)	N4−W2−Cl	84.4(2)
W1−N2−Si2	173.4(4)	N3−W2−N5	108.1(3)	N5−W2−Cl	83.2(2)
W2−N3−Si3	172.7(5)	N3−W2−Cl	164.4(3)	N4−W2−W1	123.4(2)
H1−W2−H2	104.8(40)	N4−W2−N5	82.7(3)	N5−W2−W1	121.2(2)
H1−W2−N3	95.2(24)	H1−W2−N4	155.1(26)	H1−W2−N5	79.9(27)
H1−W2−Cl	76.0(23)	H1−W2−W1	40.0(22)	H2−W2−N3	94.7(24)
H2−W2−N4	84.7(32)	H2−W2−N5	156.3(27)	H2−W2−Cl	75.7(24)
H2−W2−W1	40.8(21)	H1−W1−H2	79.4(30)	H1−W1−N1	162.3(20)
H1−W1−N2	84.0(21)	H1−W1−Cl	73.0(23)	H2−W1−N1	83.3(21)
H2−W1−N2	163.3(20)	H2−W1−Cl	74.2(24)	H1−W2−W1	54.6(25)
H2−W2−W1	52.4(29)				

[a] Terminal hydride H3 placed at d(W1−H3) = 1.673 Å, with ∠W2−W1−H3 = 76.1°, ∠H3−W1−N1 = 101.0°, ∠H3−W1−N2 = 96.5°, ∠H3−W1−N2 = 96.5°, and ∠H3−W1−Cl = 136.2°.

Table 6. Selected Interatomic Distances (Å) and Angles (deg) for (^{t}Bu$_3$SiN)$_2$WCl$_2$(py) (**6**-py)

		Interatomic Distance			
W−N1	1.747(5)		W−Cl	2.412(2)	
W−N2	2.275(7)		N1−Si1	1.746(5)	
		Angle			
N1−W−N1A	110.8(4)	N1−W−N2	124.6(2)	N2−W−Cl1	78.23(5)
N1−W−Cl	97.1(2)	Cl1−W−Cl1A	156.45(10)	W−N1−Si1	172.9(4)
N1−W−ClA	96.2(2)				

of 66.05(6)° clearly reveals the flexible nature of the chloride bridge[25] in accommodating the additional W−W and bridging hydride interactions. While the terminal hydride was not located (placed at d(W1−H3) = 1.673 Å, with ∠W2−W1−H3 = 76.1°, ∠H3−W1−N1 = 101.0°, and ∠H3−W1−N2 = 96.5°), electron density in the region anti to the pyridines and opposite the metal−metal bond from the μ-Cl was assigned to the two asymmetrically bridging hydrides. Hydrides H1 and H2 reside at 1.80(9) and 1.83(8) Å from the W(IV) center (∠H1−W2−H2 = 104.8(40)°) and 2.28(8) and 2.21(9) Å from the W(VI) core (∠H1−W1−H2 = 79.4(30)°)), respectively. The core about the W(IV) center shows the steric consequences of the bulky ^{t}Bu$_3$SiN group (∠N3−W2−N4 = 107.2(3)°, ∠N3−W2−N5 = 108.1(3)°), but the core angles are still remarkably close to that of an octahedron (∠N4−W2−N5 = 82.7(3)°, ∠N4−W2−Cl = 84.4(2)°, and ∠N5−W2−Cl = 83.2(2)°). While angles involving the hydrides must be assessed with care, all are within reason for a pseudo-octahedral environment, as Table 5 indicates.

4. Structure of (^{t}Bu$_3$SiN)$_2$WCl$_2$(py) (6-py). Confirmation of the pseudo-tbp structure[26] of (^{t}Bu$_3$SiN)$_2$WCl$_2$(py) (**6**-py) was obtained via a single-crystal X-ray structure determination (Table 2, Table 6, Figure 4). Crystallographically equivalent, bulky ^{t}Bu$_3$SiN groups (d(WN) = 1.747(5) Å; ∠N1−W−N1A = 110.8(4)°) and the pyridine occupy equatorial positions (d(WN) = 2.275(7) Å; ∠N1−W−N2 = 124.6(2)°). Crystallographically equivalent chlorides are axial (d(W−Cl) = 2.412(2) Å) and manifest a decided "lean" away from the imides

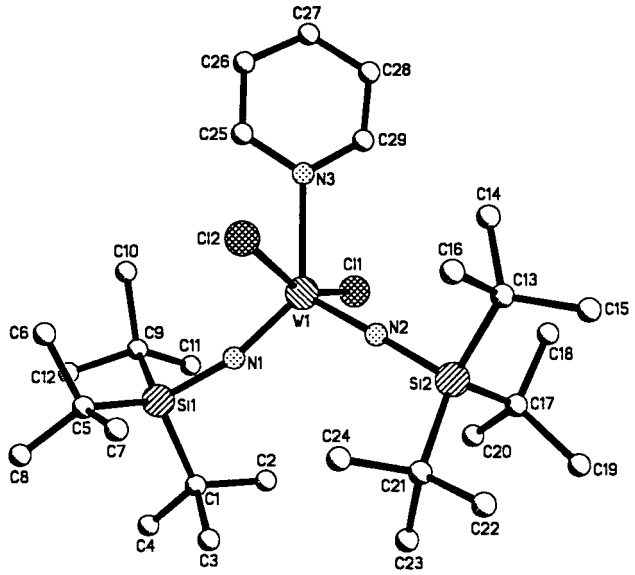

Figure 4. Molecular structure of (^{t}Bu$_3$SiN)$_2$WCl$_2$(py) (**6**-py).

(∠Cl−W−N = 97.1(2)°, 96.2(2)°; ∠Cl1−W−Cl1A = 156.45(10)°) and toward the py (∠Cl−W−N = 78.2(1)°) reminiscent of the distortions in pseudo-tbp (^{t}Bu$_3$SiN)$_2$Tapy$_2$-(Me).[21,22] While it is tempting to conclude these features are steric in origin, recent arguments suggest that second-order Jahn−Teller effects are responsible[27] and provide a rationale for the curiously small ∠N1−W−N1A angle.

Olefin Trapping of Putative "(^{t}Bu$_3$SiN)$_2$WHCl" (4). 1. ^{t}BuCH=CH$_2$. If the thermal decomposition of (^{t}Bu$_3$SiNH)$_2$Cl-

(25) (a) Summerville, R. H.; Hoffmann, R. *J. Am. Chem. Soc.* **1979**, *101*, 3821−3831. (b) Summerville, R. H.; Hoffmann, R. *J. Am. Chem. Soc.* **1976**, *98*, 7240−7255.

(26) Bradley, D. C.; Errington, R. J.; Hursthouse, M. B.; Short, R. L.; Ashcroft, B. R.; Clark, G. R.; Nielson, A. J.; Rickard, C. E. F. *J. Chem. Soc., Dalton Trans.* **1987**, 2067−2075.

(27) Ward, T. R.; Burgi, H. B.; Gilardoni, P.; Weber, J. *J. Am. Chem. Soc.* **1997**, *119*, 11974−11985.

Scheme 2

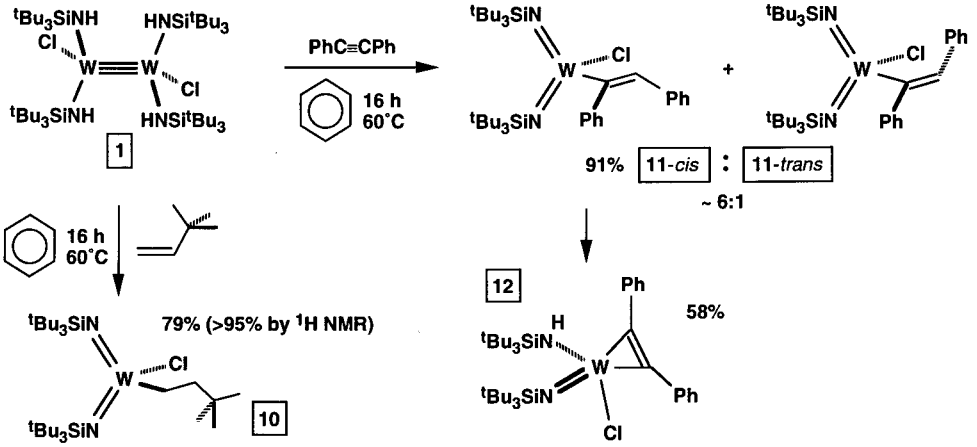

Table 7. Selected Interatomic Distances (Å) and Angles (deg) for (^{t}Bu$_3$SiN)$_2$WCl(*trans*-CPh═CPhH) (**11**-*trans*)

		Interatomic Distance			
W−N1	1.759(10)	W−Cl	2.296(3)	W−C25	2.16(2)
W−N2	1.783(11)	N1−Si1	1.766(11)	N2−Si2	1.735(12)
C25−C32	1.24(4)				
		Angle			
N1−W−N2	111.8(5)	N1−W−Cl	108.3(3)	N2−W−Cl	104.5(3)
N1−W−C25	108.1(6)	N2−W−C25	111.1(8)	Cl−W−C25	113.0(9)
W−C25−C32	148.5(29)	W−C25−C26	95.7(8)	C25−C32−C33	133.9(26)
W−N1−Si1	174.8(7)	W−N2−Si2	167.2(6)		

W≡WCl(NHSi^{t}Bu$_3$)$_2$ (**1**) is undertaken with hydride scavengers present, evidence for the putative intermediate "(^{t}Bu$_3$SiN)$_2$WHCl" (**4**) or related precursor hydrides is corroborated, as Scheme 2 shows. Thermolysis of **1** (60 °C, 16 h) in benzene-d_6 with ∼5 equiv of ^{t}BuCH═CH$_2$ afforded (^{t}Bu$_3$SiN)$_2$W(^{neo}Hex)Cl (**10**) in 95% yield, and scale-up of the reaction enabled isolation of **10** in 79% yield as waxy, yellow-brown crystals. Methylene resonances are observed at δ 2.08 and 2.65 in the ^{1}H NMR spectrum, as are equivalent imido groups.

When diphenyl acetylene was used as the scavenger under standard degradation conditions (16 h, 60 °C), a ∼6:1 mixture of cis and trans insertion products, (^{t}Bu$_3$SiN)$_2$WCl(*cis*-CPh═CPhH) (**11**-*cis*) and (^{t}Bu$_3$SiN)$_2$WCl(*trans*-CPh═CPhH) (**11**-*trans*), was isolated as a yellow-brown oil in 91% yield from pentane; in a related 24 h thermolysis (60 °C), the minor trans isomer was crystallized from THF/MeCN in 16% yield. Because NMR spectral studies failed to distinguish their structures (e.g., **11**-*cis*, $^3J_{WH}$ = 7.6 Hz; **11**-*trans*, $^3J_{WH}$ = 8.4 Hz), structure proof of **11**-*trans* was obtained via single-crystal X-ray diffraction. Elevated temperatures (4 d, 150 °C) effected further isomerization of **11**-*cis* to amber, crystalline (^{t}Bu$_3$SiNH)(^{t}Bu$_3$SiN)WCl-(η^2-PhCCPh) (**12**) in 64% yield according to ^{1}H NMR analysis (58% isolated yield). A few percent (18%) of **11**-*cis* and **11**-*trans* remained in solution along with some evidence of degradation (∼10% ^{t}Bu$_3$SiNH$_2$ and trace unknown products). Distinct ^{1}H and ^{13}C{^{1}H} NMR resonances for the amide and imide groups, signals for two Ph groups, an NH resonance at δ 8.08, and a corresponding ν(NH) at 3263 cm^{-1} characterize **12**, whose structure was confirmed by single-crystal X-ray crystallography. ^{13}C{^{1}H} NMR spectral resonances at δ 175.08 and 189.80 suggest that the diphenylacetylene may be considered a 4 e$^-$ donor.[28] Mechanisms that lead to **12** would more logically proceed via **11**-*cis*, because the activated β-H is directed toward W in this structure; hence, it is portrayed as the precursor.

(28) Templeton, J. L. *Adv. Organomet. Chem.* **1989**, *29*, 1−100.

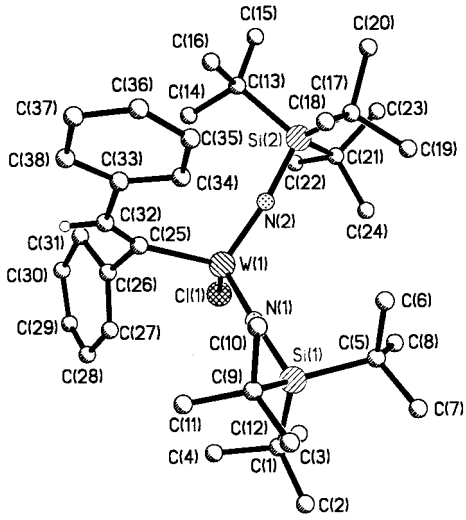

Figure 5. Molecular structure of (^{t}Bu$_3$SiN)$_2$WCl(*trans*-CPh═CPhH) (**11**-*trans*).

2. Structure of (^{t}Bu$_3$SiN)$_2$WCl(*trans*-CPh═CPhH) (11-*trans*). Despite a mediocre data set, an X-ray structure determination (Table 2) identified (^{t}Bu$_3$SiN)$_2$WCl(*trans*-CPh═CPhH) (**11**-*trans*) as the minor isomer in the above thermolysis. A pseudotetrahedral environment about the tungsten is observed (109.5(31)° av core angle), along with normal bond distances: d(WN) = 1.759(10), 1.783(11) Å; d(WC) = 2.16(2) Å; d(WCl) = 2.296(3) Å (Table 7, Figure 5). The alkenyl C═C bond is 1.24(4) Å, and the ∠W−C25−C32 and ∠C25−C32−C33 angles are opened up to 148.5(29)° and 133.9(26)°, respectively, presumably as a consequence of steric interations. While an ortho hydrogen of the β-phenyl group, whose ring plane is oriented between the bulky imido ligands, is 3.22 Å away from the tungsten, no core distortions are evident. The α-phenyl ring is rotated perpendicular to the alkenyl plane, and while ∠C26−C25−C32 = 115.9(28)° is normal, the accompanying W−C25−

Table 8. Selected Interatomic Distances (Å) and Angles (deg) for (^{t}Bu$_3$SiNH)(^{t}Bu$_3$SiN)WCl(PhCCPh) (**12**)

		Interatomic Distance			
W−N1	1.906(4)	W−C25	2.073(4)	W−Cl	2.3386(13)
W−N2	1.758(4)	W−C26	2.063(4)	C25−C26	1.315(6)
N1−Si1	1.762(4)	N2−Si2	1.754(4)		
		Angle			
N1−W−N2	107.65(19)	N1−W−Cl	108.53(13)	N2−W−Cl	103.82(13)
N1−W−C25	127.11(17)	N1−W−C26	108.82(16)	Cl−W−C25	86.84(13)
N2−W−C25	117.41(17)	N2−W−C26	102.93(16)	Cl−W−C26	123.88(13)
C25−W−C26	37.06(17)	C25−C26−C27	139.3(4)	C26−C25−C33	142.0(4)
W−C25−C26	71.0(3)	W−C26−C25	71.9(3)	W−C25−C33	147.0(3)
W−N1−Si1	150.3(3)	W−N2−Si2	171.4(3)	W−C26−C27	147.2(3)

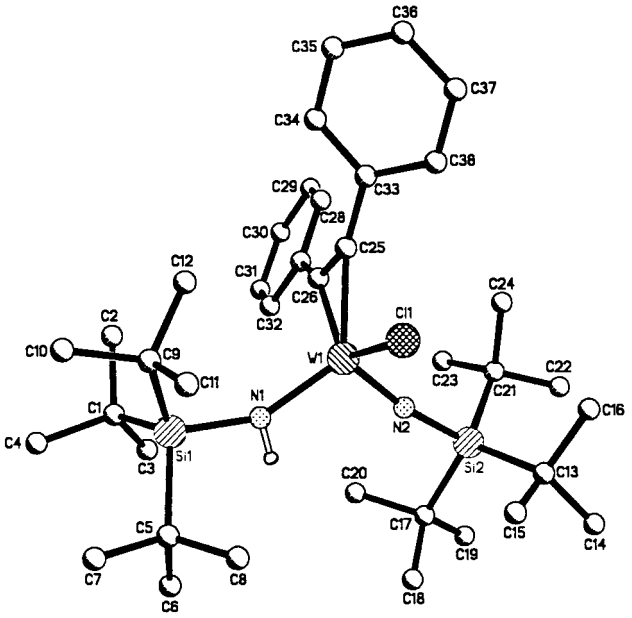

Figure 6. Molecular structure of (^{t}Bu$_3$SiNH)(^{t}Bu$_3$SiN)WCl(η^2-PhC-CPh) (**12**).

C26 angle is 95.7(8)°; thus, the alkenyl group as a whole is rotated in response to the steric interactions. As a consequence, the Cl is only 3.36 Å from the α-phenyl ring centroid.

3. Structure of (^{t}Bu$_3$SiNH)(^{t}Bu$_3$SiN)WCl(η^2-PhCCPh) (12). The lack of definitive NMR spectroscopic handles on the proposed alkyne complex, (^{t}Bu$_3$SiNH)(^{t}Bu$_3$SiN)WCl(η^2-PhC-CPh) (**12**), prompted a single-crystal X-ray diffraction study (Table 2). Normal imide (1.758(4) Å), amide (1.906(4) Å), and chloride (2.3386(13) Å) bond distances accompany a symmetrically bound diphenylacetylene (2.063(4), 2.073(4) Å) about the tungsten (Table 8, Figure 6). The amide ligand, because of its W−N−Si angle of 150.3(3)° and orientation that places the bulk of the ^{t}Bu$_3$Si group away from the imide (∠(H)N−W−N = 107.65(19)°), exerts a steric influence that is modestly greater than that of the imide. Core angles (H)N−W−C$_2$(midpoint) = 118.0(2)° and (H)N−W−Cl = 108.53(13)° are slightly greater than the corresponding angles pertaining to the imide, which are 107.7(2)° and 103.82(13)°. As in (^{t}Bu$_3$SiN)$_2$WCl(*trans*-CPh=CPhH) (**11**-*trans*), the plane of one phenyl group is oriented between the amide and imide, and its ortho H is 3.67 Å from the tungsten. The interior ring is roughly perpendicular to the W(alkyne) plane, presumably to minimize the interaction with the adjacent chloride (∠ClWC25 = 86.84(13)°, ∠ClWC26 = 123.88(13)°), which is 4.40 Å from its centroid. Significant back-bonding by the formally W(IV) metal center is indicated by the rather long diphenylacetylene CC bond (1.315(6) Å) and C25−C26−C27 and C26−C25−C33 angles of 139.3(4)° and 142.0(4)°, respectively.

Alkylation of (^{t}Bu$_3$SiNH)$_2$ClW≡WCl(NHSi^{t}Bu$_3$)$_2$ (1). To probe related degradations, alkylation of [(^{t}Bu$_3$SiNH)$_2$WCl]$_2$ (**1**) was sought as a route to a corresponding ditungsten dimethyl derivative akin to [(^{t}Bu$_3$SiO)$_2$WMe]$_2$, which is prepared upon methylation of [(^{t}Bu$_3$SiO)$_2$WCl]$_2$.[12] Instead, treatment of **1** with MeMgBr (optimized at 6 equiv) in Et$_2$O at −72 °C afforded yellow (^{t}Bu$_3$SiN)$_2$W(CH$_3$)$_2$ (**13**) in 25% yield based on tungsten (eq 9).

$$\underset{\mathbf{1}}{[(^t\mathrm{Bu_3SiNH})_2\mathrm{WCl}]_2} + \text{excess MeMgBr} \xrightarrow[-72°,\ 6\mathrm{h};\ 23\ °\mathrm{C},\ 16\mathrm{h}]{\mathrm{Et_2O}} \underset{\mathbf{13}}{(^t\mathrm{Bu_3SiN})_2\mathrm{W(CH_3)_2}} + \ldots \quad (9)$$

$$\underset{\mathbf{6}}{(^t\mathrm{Bu_3SiN})_2\mathrm{WCl_2}} + 2\ \mathrm{MeMgBr} \xrightarrow[-72°,\ 1\mathrm{h}]{\mathrm{Et_2O}} \underset{\mathbf{13}}{(^t\mathrm{Bu_3SiN})_2\mathrm{W(CH_3)_2}} + 2\ \mathrm{MgBrCl} \quad (10)$$

The mononuclear dimethyl was readily characterized by a singlet at δ 1.17 accompanied by satellites ($^2J_{WH}$ = 9 Hz, 14%) in its ^{1}H NMR spectrum and equivalent imido groups. In support, treatment of (^{t}Bu$_3$SiN)$_2$WCl$_2$ with 2 equiv of MeMgBr generated **13** in 59% isolated yield (eq 10) under similar conditions.

Discussion

Generalization. Upon examination of the degradation and derivatization studies involving (^{t}Bu$_3$SiNH)$_2$ClW≡WCl(NHSi-^{t}Bu$_3$)$_2$ (**1**), a cogent pattern emerges, as Scheme 3 elucidates. NH bond activation[29,30] by the W≡W bond initiates a degradation cascade that produces a double-bonded dinuclear complex containing an imide and a hydride, depicted as **I**. Alternatively, when a donor ligand is present, 1,2-elimination of amine[31−34] can lead to the imido dinclear species **II** whose W≡W bond is retained. Subsequent NH activation events (**I** → **III**) lead to

(29) For NH bond activation involved in a catalytic C−N bond forming reaction, see: (a) Johnson, J. S.; Bergman, R. G. *J. Am. Chem. Soc.* **2001**, *123*, 2923−2924. (b) Walsh, P. J.; Baranger, A. M.; Bergman, R. G. *J. Am. Chem. Soc.* **1992**, *114*, 1708−1719.

(30) For NH bond activation involved in a catalytic C−N bond forming reaction, see: (a) Li, Y.; Marks, T. J. *J. Am. Chem. Soc.* **1998**, *120*, 1757−1771. (b) Arredondo, V. M.; Tian, S.; McDonald, F. E.; Marks, T. J. *J. Am. Chem. Soc.* **1999**, *121*, 3633−3639.

(31) Zambrano, C. H.; Profilet, R. D.; Hill, J. E.; Fanwick, P. E.; Rothwell, I. P. *Polyhedron* **1993**, *12*, 689−708.

(32) Arney, D. J.; Bruck, M. A.; Huber, S. R.; Wigley, D. E. *Inorg. Chem.* **1992**, *31*, 3749−3755.

(33) Cummins, C. C.; Schaller, C. P.; Van Duyne, G. D.; Wolczanski, P. T.; Chan, E. A.-W.; Hoffmann, R. *J. Am. Chem. Soc.* **1991**, *113*, 2985−2994.

(34) (a) Bonanno, J. B.; Wolczanski, P. T.; Lobkovsky, E. B. *J. Am. Chem. Soc.* **1994**, *116*, 11159−11160. (b) Bonanno, J. B.; Henry, T. P.; Neithamer, D. R.; Wolczanski, P. T.; Lobkovsky, E. B. *J. Am. Chem. Soc.* **1996**, *118*, 5132−5133.

Scheme 3

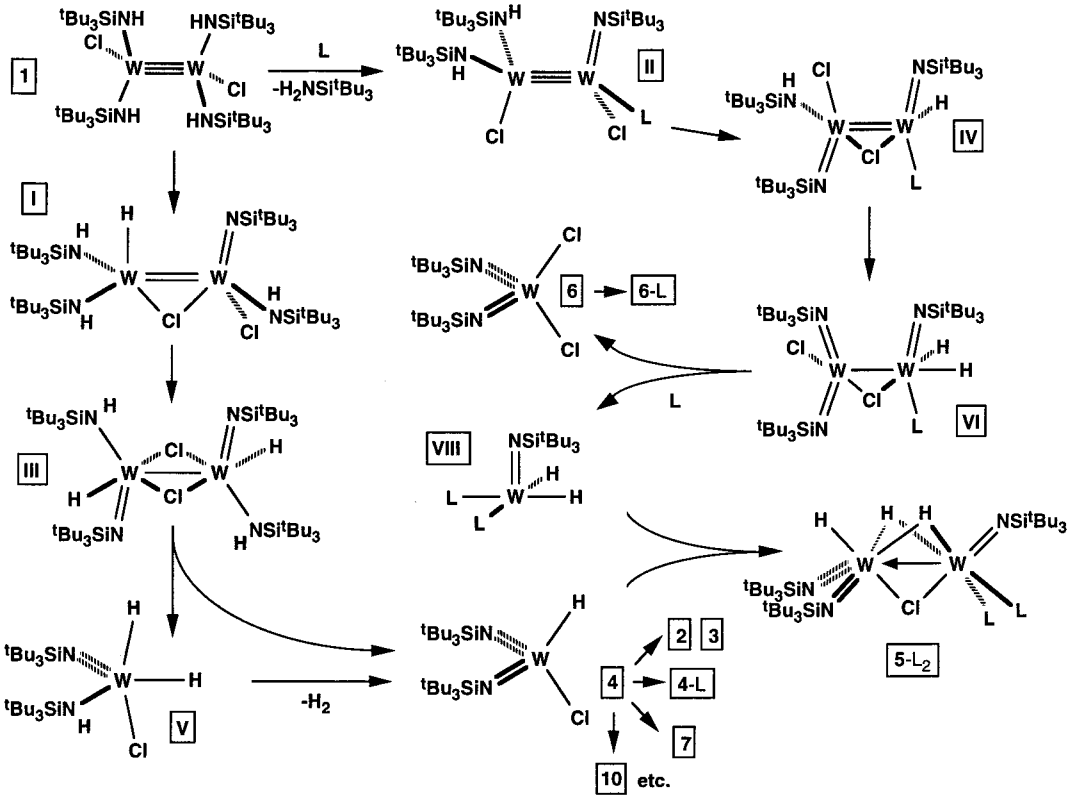

the cleavage of the ditungsten unit to afford "(^{t}Bu$_3$SiN)$_2$WHCl" (**4**) and (^{t}Bu$_3$SiN)(^{t}Bu$_3$SiNH)WH$_2$Cl (**V**), which is a precursor to **4** as a consequence of 1,2-H$_2$-elimination or H$_2$ reductive elimination followed by NH α-elimination.[35] The putative hydrido chloride (**4**) may then be converted to various derivatives depending on the conditions. It is interesting that while 1,2-NH-elimination/addition pathways are responsible for the creation of imido ligands in many d^0 systems,[31−34] discrete cases of NH α-elimination on single or multiple metal centers are rare.

The pathway emanating from 1,2-amine-elimination provides trihydrides (^{t}Bu$_3$SiN)$_2$HW(μ-Cl)(μ-H)$_2$W(NSi^{t}Bu$_3$)L$_2$ (**5**-L$_2$; L$_2$ = py$_2$, DME) and dichloride (^{t}Bu$_3$SiN)$_2$WCl$_2$ (**6**), as another NH bond activation sequence (**II** → **IV** → **VI**) leads to tungsten−tungsten bond scission. The direct generation of **6** from **VI** is accompanied by the stabilization of an imido−dihydride moiety as a solvent adduct, (^{t}Bu$_3$SiN)WH$_2$L$_n$ (**VIII**), and this species should be electrophilic enough to trap "(^{t}Bu$_3$SiN)$_2$WHCl" (**4**) to afford trihydrides **5**-L$_2$.

Rationale. While alternative paths cannot be discounted on the basis of the product analyses herein, Scheme 3 protrays plausible sequences containing the minimum number of steps that lead to the observed products. Proposed intermediates **I**−**VI** and **VIII** may also possess different configurations from those presented, but the essential transformations are unlikely to be substantially different. In donor solvents, decomposition paths lead to products that can all be accounted for via sequential NH activation events centered on the ditungsten unit. In pyridine, the sequences in Scheme 3 account for ∼70% of the total tungsten in Scheme 2. Moreover, the amount of amine released as ^{t}Bu$_3$SiNH$_2$ and ^{t}Bu$_3$SiNH$_3^+$(presumably with Cl$^-$ counterion) is approximately the same as the amount of tungsten in (^{t}Bu$_3$SiN)$_2$WCl$_2$py (**6**-py) and (^{t}Bu$_3$SiN)$_2$HW(μ-Cl)(μ-H)$_2$W(NSi^{t}Bu$_3$)L$_2$ (**5**-py$_2$) that is derived from the py-induced amine elimination path. Similarly, the amount of tungsten in (^{t}Bu$_3$SiN)$_2$WCl$_2$ (**6**) and (^{t}Bu$_3$SiN)$_2$HW(μ-Cl)(μ-H)$_2$W(NSi^{t}Bu$_3$)L$_2$ (**5**-DME) generated in DME is similar to the amount of amine (as neutral and cation) released, as predicted by Scheme 3.

Given the isolation of (^{t}Bu$_3$SiN)$_2$WHCl(py) (**4**-py) and (^{t}Bu$_3$SiN)$_2$HW(μ-Cl)(μ-H)$_2$W(NSi^{t}Bu$_3$)L$_2$ (**5**-L$_2$; L$_2$ = py$_2$, DME), it is somewhat surprising that degradations in nondonor solvents led to intractable mixtures and a substantial quantity of free amine. However, an aggregate such as [(^{t}Bu$_3$SiN)$_2$WHCl]$_n$ (**4**$_n$) was not observed, thus suggesting that any form of the hydridochloride is subject to ligand loss in the absence of donor solvents that stabilize it or reagents that trap the hydride. Instead, evidence for **4** is indirect yet considerable and rests with a set of derivatives that are generated under various conditions: (1) the major product in pyridine is **4**-py; (2) the major product in DME is (^{t}Bu$_3$SiN)$_2$WCl(OMe) (**7**), a product obtained from hydride attack on the solvent; (3) the minor trihydride products **5**-L$_2$ (L$_2$ = py$_2$, DME) contain the hydridochloride moiety; (4) the presence of H$_2$C═CH^{t}Bu and PhC≡CPh leads to remarkably efficient hydride scavenging to produce (^{t}Bu$_3$SiN)$_2$W(^{neo}Hex)Cl (**10**) and (^{t}Bu$_3$SiN)$_2$WCl(*cis*-CPh═CPhH) (**11**-*cis*), respectively; and (5) the synthesis of (^{t}Bu$_3$SiN)$_2$(^{t}Bu$_3$SiNH)WH (**2**) and (^{t}Bu$_3$SiN)$_2$(^{t}Bu$_3$SiO)WH (**3**) may be rationalized by attack of ^{t}Bu$_3$SiZ$^-$ (Z = O, NH) on "(^{t}Bu$_3$SiN)$_2$WHCl" (**4**). It is also plausible that donor solvents, ^{t}Bu$_3$SiZ$^-$ (Z = O, NH), and the olefins intercept earlier hydride intermediates (e.g., **I**, **III**) and funnel the degradation toward isolable products. For example, note the mild conditions which permit the synthesis of (^{t}Bu$_3$SiN)$_2$W(CH$_3$)$_2$ (**13**) from [(^{t}Bu$_3$SiNH)$_2$WCl]$_2$ (**1**), which suggest that NH activations leading to W≡W bond scission may speed up upon metathesis of Cl$^-$ with Me$^-$. However, the simplest way to envision the majority of the transformations (e.g., 1−5 above), which occur under more severe conditions, is to consider

(35) Trinquier, B.; Hoffmann, R. *Organometallics* **1984**, *3*, 370−380.

the direct reaction of transient "(^{t}Bu$_3$SiN)$_2$WHCl" (**4**). It is also noteworthy that no (^{t}Bu$_3$SiN)$_2$(^{t}Bu$_3$SiNH)WX derivatives,[11] which are extremely thermally and kinetically stable, were identified in any degradations.

Summary. The bulk of the primary amide, ^{t}Bu$_3$SiNH, hinders NH activation paths that eventually decompose (^{t}Bu$_3$SiNH)$_2$ClW≡WCl(NHSi^{t}Bu$_3$)$_2$ (**1**). Related dinuclear species that feature secondary amide ligands have substantially greater thermal stability, while smaller primary amide-containing metal−metal triply bonded species do not exist. Through mass balance and the isolation and identification of primary and "scavenged" degradation products, the decomposition of **1** is most simply considered as a series of NH activations by the W≡W unit to afford the penultimate intermediate, "(^{t}Bu$_3$SiN)$_2$WHCl" (**4**).

Experimental Section

General Considerations. All manipulations were performed using glovebox or high vacuum techniques. Hydrocarbon and ethereal solvents were dried over and vacuum transferred from purple sodium benzophenone ketyl (with 3−4 mL tetraglyme/L added to hydrocarbons). Benzene-d_6 was sequentially dried over sodium and 4 Å molecular sieves and then stored over and vacuum transferred from sodium benzophenone ketyl. All glassware was base-washed and oven-dried. NMR tubes for sealed tube experiments were flame-dried under dynamic vacuum prior to use. Organic reagents and solutions of lithium alkyls were obtained from Aldrich Chemical. NaW$_2$Cl$_7$(THF)$_5$[7] and ^{t}Bu$_3$SiNHLi[10] were prepared according to literature procedures.

^{1}H, ^{13}C{^{1}H}, and ^{2}H{^{1}H] NMR spectra were obtained using Varian XL-200, XL-400, and Unity-500 spectrometers. Infrared spectra were recorded on a Nicolet Impact 410 spectrophotometer interfaced to a Gateway PC. Combustion analyses were performed by Oneida Research Services, Whitesboro, NY, or Robertson Microlit Laboratories, Madison, NJ.

Procedures. 1. [(^{t}Bu$_3$SiNH)$_2$WCl]$_2$ (1). To a glass bomb reactor containing NaW$_2$Cl$_7$(THF)$_5$ (400 mg, 0.400 mmol) and ^{t}Bu$_3$SiNHLi (400 mg, 1.81 mmol, 4.5 equiv) was transferred 10 mL of benzene via vacuum transfer. The vessel warmed to room temperature and was stirred at 23 °C until the green color had faded (∼55 min) and the solution became brown. After removal of all volatiles, the remaining solids were triturated with hexanes two times and filtered to remove salt byproduct. The solution volume was reduced to 4 mL and cooled to −78 °C, producing 250 mg orange-brown **1** (48%) which was collected by filtration. Elemental analysis was not attempted, because some solid-state decomposition (23 °C) was noted after a few days.

2. (^{t}Bu$_3$SiN)$_2$(^{t}Bu$_3$SiNH)WH (2). To a glass bomb reactor containing NaW$_2$Cl$_7$(THF)$_5$ (6.01 g, 6.01 mmol) and ^{t}Bu$_3$SiNHLi (8.46 g, 38.2 mmol) was transferred 100 mL of benzene. The vessel warmed to 23 °C and was stirred at room temperature until the green color had faded (∼45 min) and the solution became brown. All volatiles were removed in vacuo, and fresh benzene (200 mL) was distilled into the reaction mixture. The bomb was immersed in a 100 °C bath for 6 h, and the volatiles were removed. The reaction mixture was taken up in hexane and filtered and the white residue slurried in 30 mL THF at −78 °C and filtered to separate **1**-H (5.42 g) from the brown solution in 55% isolated yield. In a separate experiment, all volatiles removed from the reaction vessel were passed through three LN$_2$ traps, and 0.78 equiv of H$_2$ (^{1}H NMR: δ 4.46 ppm) per equiv of NaW$_2$Cl$_7$(THF)$_5$ was collected by Toepler pump. Anal. Calcd for C$_{36}$H$_{83}$N$_3$Si$_3$W: C, 52.34; H, 10.13; N, 5.09. Found: C, 51.71; H, 10.53; N, 5.01.

3. (^{t}Bu$_3$SiO)Tl. To a flask containing TlOEt (5.1 g, 22.6 mmol) and ^{t}Bu$_3$SiOH (4.94 g, 22.7 mmol) was added 40 mL of THF via vacuum transfer. The mixture was allowed to warm to 23 °C and stirred for an additional 30 min. The mixture was evacuated to dryness, yielding an opaque, gelatinous mass. The residue was triturated three times with hexanes (30 mL) and dissolved in 40 mL of hexanes. The mixture was filtered and the filtrate concentrated to 15 mL and cooled to −78 °C. The white solid obtained upon cold filtration was dried under vacuum at 23 °C to afford 7.43 g (78%) of (^{t}Bu$_3$SiO)Tl. ^{1}H NMR (C$_6$D$_6$): δ 1.21 (s); ^{13}C{^{1}H} NMR: δ 24.01 (CMe$_3$), 31.45 (CH$_3$).

4. (^{t}Bu$_3$SiN)$_2$(^{t}Bu$_3$SiO)WH (3). To a glass bomb reactor containing NaW$_2$Cl$_7$(THF)$_5$ (308 mg, 0.308 mmol) and ^{t}Bu$_3$SiNHLi (280 mg, 1.26 mmol) was transferred 10 mL of benzene. The vessel warmed to 23 °C and was stirred for 45 min, as above. After removal of all volatiles, TlOSi^{t}Bu$_3$ (330 mg, 0.308 mmol) was loaded into the reaction vessel followed by 20 mL of THF. The reaction was stirred for 5 h at 0 °C and 8 h at 60 °C. After removal of all volatiles and filtration in hexane, the solution volume was reduced to 3 mL and cooled to −78 °C, precipitating a light yellow powder that was collected by filtration to yield 135 mg (^{t}Bu$_3$SiN)$_2$(^{t}Bu$_3$SiO)WH (53%). Anal. Calcd for C$_{36}$H$_{82}$N$_2$OSi$_3$W: C, 52.27; H, 9.99; N, 3.39. Found: C, 51.92; H, 9.77; N, 3.72.

5. (^{t}Bu$_3$SiN)$_2$WHCl(py) (4-py). To a flask containing **1** (375 mg, 289 mmol) and 3 mL of pyridine was added 40 mL of benzene. The mixture was stirred for 16 h at 60 °C. The dark purple solution was evacuated to dryness, and the residue was triturated three times with pentane (5 mL). The purple residue was washed with pentane and filtered. The filtrate volume was reduced to 2 mL and deposited **4**-py as white crystals (118 mg, 28%). Anal. Calcd for C$_{30}$H$_{60}$N$_3$Si$_2$ClW: C, 47.91; H, 8.34; N, 5.78. Found: C, 47.44; H, 8.07; N, 5.58.

6. (^{t}Bu$_3$SiN)$_2$HW(μ-Cl)(μ-H)$_2$W(NSi^{t}Bu$_3$)py$_2$ (5-py$_2$). To a flask containing **1** (375 mg, 0.289 mmol) and 3 mL of pyridine was added 40 mL of benzene. The mixture was stirred for 16 h at 60 °C. The dark purple solution was evacuated to dryness, and the residue was triturated three times with pentane (5 mL). The purple residue was washed with pentane and filtered. The filtrate volume was reduced to 2 mL and deposited **4**-py as white crystals. After three crystallizations, **5**-py$_2$ was obtained as dark purple crystals (25 mg).

7. (^{t}Bu$_3$SiN)$_2$WCl$_2$ (6). A flask containing **1** (386 mg, 0.298 mmol) and SnCl$_4$(THF)$_2$ (120 mg, 0.297 mmol) in 20 mL of benzene was stirred for 16 h at 60 °C. The yellow-green mixture was evacuated to dryness, and the residue was triturated three times with pentane (5 mL). The yellow-green residue was washed with pentane and filtered through Celite until a colorless filtrate was obtained. The filtrate was dried under vacuum, yielding yellow microcrystals of **6** (205 mg, 50%). In a separate experiment attached to a Toepler pump, 0.95 equiv H$_2$ (vs **1**) was released. Anal. Calcd for C$_{24}$H$_{54}$N$_2$Si$_2$Cl$_2$W: C, 42.25; H, 8.00; N, 4.11. Found: C, 41.55; H, 7.86; N, 3.84.

8. (^{t}Bu$_3$SiN)$_2$WCl$_2$(py) (6-py). When **6** was recrystallized from pyridine, **6**-py was generated. Anal. Calcd for C$_{29}$H$_{59}$N$_3$Si$_2$Cl$_2$W: C, 45.75; H, 7.83; N, 5.52. Found: C, 44.63; H, 7.73; N, 5.17.

9. (^{t}Bu$_3$SiN)$_2$WCl(OMe) (7). A flask containing **1** (430 mg, 0.332 mmol) and 10 mL of DME was magnetically stirred for 16 h at 55 °C. The orange-brown solution was concentrated to 4 mL and filtered. The volatiles were removed, and the solid was triturated three times with pentane (5 mL) and dried under vacuum at 23 °C for 6 h. The solid was dissolved in Et$_2$O, filtered, and concentrated to 2 mL. Upon cooling to −20 °C, pale yellow crystals of **7** were isolated (76 mg, 17%). Anal. Calcd for C$_{25}$H$_{57}$N$_2$Si$_2$ClOW: C, 44.70; H, 8.58; N, 4.17. Found: C, 42.97; H, 8.24; N, 4.13.

10. (^{t}Bu$_3$SiN)$_2$(^{t}Bu$_3$SiNH)WO^{n}Bu (8). A glass reaction vessel was charged with **1**-H (501 mg, 6.06 × 10^{-4} mol) followed by 30 mL of THF, and the solution was stirred at 145 °C for 25 h followed by removal of all volatiles. The residue was taken up in hexanes and transferred into a frit assembly for workup. Four milliliters of bistrimethylsilyl ether was vacuum transferred onto the remaining material, and this suspension was heated to 70 °C for 1 h, over which time all material dissolved. The solution was allowed to slowly cool to 23 °C, and after 30 min, yellow crystals had formed. The flask was cooled to 0 °C for an additional 30 min, and the crystals were collected by filtration, yielding 280 mg **1**-O^{n}Bu (51%).

11. (^{t}Bu$_3$SiN)$_2$W(^{neo}Hex)Cl (10). To a flask containing **1** (367 mg, 0.283 mmol) and 30 mL of benzene was added an excess of 3,3′-dimethyl-1-butene (2 mL, 16 mmol). The mixture was stirred for 16 h at 60 °C. The yellow-brown solution was evacuated to dryness, and the residue was triturated three times with pentane (5 mL). The residue was washed with pentane and filtered through Celite until a colorless filtrate was obtained. The filtrate was evacuated to dryness and afforded **10** as a viscous yellow-brown oil (393 mg, 95%). Waxy crystals were obtained by dissolving the brown oil in a minimum of 1:5 Et$_2$O/TMS$_2$O at 23 °C. Decanting the mother liquor and drying the

crystals at 60 °C under vacuum 12 h afforded **10** (325 mg, 79%). Anal. Calcd for $C_{30}H_{65}N_2Si_2ClW$: C, 49.22; H, 9.25; N, 3.83. Found: C, 48.54; H, 9.06; N, 3.79.

12. (^{t}Bu$_3$SiN)$_2$WCl(*cis*-CPh=CPhH) (11-*cis*). To a flask containing **1** (500 mg, 0.386 mmol) and Ph_2C_2 (137 mg, 0.769 mmol) was added 40 mL of benzene. The mixture was stirred for 16 h at 60 °C, and the yellow-brown solution was evacuated to dryness. The remaining yellow-brown oil was triturated three times with pentane (5 mL). The residue was washed with pentane and filtered through Celite until a colorless filtrate was obtained. The filtrate was evacuated to dryness and afforded a 6:1 mixture of **11**-*cis*:**11**-*trans* as a viscous yellow-brown oil (594 mg, 91%). Anal. Calcd for $C_{38}H_{65}N_2Si_2ClW$: C, 55.24; H, 7.95; N, 3.39. Found: C, 55.92; H, 8.07; N, 3.27.

13. (^{t}Bu$_3$SiN)$_2$WCl(*trans*-CPh=CPhH) (11-*trans*). A flask containing **1** (1.009, 0.778 mmol) and Ph_2C_2 (277 mg, 1.56 mmol) in 40 mL of benzene was stirred for 24 h at 65 °C. The yellow-brown solution was evacuated to dryness, and the yellow-brown residue was triturated three times with pentane (5 mL). The solid was dissolved in a minimum amount of THF, and acetonitrile was added until a brown oil began to form. Crystallization and recrystallization from THF/MeCN afforded **11**-*trans* as a yellow-brown solid (210 mg, 16%).

14. (^{t}Bu$_3$SiNH)(^{t}Bu$_3$SiN)WCl(η^2-PhCCPh) (12). A flask containing **11**-*cis*:**11**-*trans* (400 mg, 0.485 mmol) and 7 mL of benzene was stirred for 16 h at 150 °C. The yellow-brown solution was evacuated to dryness, and the residue was triturated three times with pentane (2 mL). The yellow-brown residue was extracted into a minimum of benzene and allowed to stand at 23 °C overnight under a slight vacuum. The mother liquor was decanted, and crystals were dried for 1 h under vacuum at 23 °C to yield 232 mg of **12** (58% yield). Anal. Calcd for $C_{38}H_{65}N_2Si_2ClW$: C, 55.31; H, 7.96; N, 3.40. Found: C, 55.96; H, 7.96; N, 3.27.

15. (^{t}Bu$_3$SiN)$_2$W(CH$_3$)$_2$ (13). a. Into a flask containing **1** (688 mg, 0.531 mmol) in 75 mL of Et_2O was syringed a solution of CH_3MgBr (3.0 M in Et_2O, 1.06 mL, 3.18 mmol). The mixture was stirred for 6 h at −72 °C and was allowed to slowly warm to 23 °C over 16 h. The yellow mixture was evacuated to dryness, and the pale yellow residue was triturated three times with pentane (5 mL). The yellow solid was washed with pentane and filtered through Celite until a colorless filtrate was obtained. The filtrate was evacuated to dryness yielding **13** as a yellow solid (170 mg, 25% based on W).

b. Into a 15 mL Et_2O solution of (^{t}Bu$_3$SiN)$_2$WCl$_2$ (**6**) (160 mg, 0.235 mmol) was syringed a solution of CH_3MgBr (3.0 M in Et_2O, 0.16 mL, 0.494 mmol) at −72 °C. The yellow mixture was stirred for 1 h at −72 °C, and the resulting yellow mixture was evacuated to dryness. The pale yellow residue was triturated three times with pentane (5 mL) and was filtered through Celite. The salt cake was washed with pentane until a colorless filtrate was obtained. The filtrates were evacuated to dryness yielding **13** as a yellow solid (89 mg, 59%). Anal. Calcd for $C_{26}H_{60}N_2Si_2W$: C, 48.69; H, 9.46; N, 4.37. Found: C, 48.61; H, 9.26; N, 3.87.

NMR Tube Reactions. General. Flame dried NMR tubes, sealed to 14/20 ground glass joints, were charged with metal reagent (typically 10 mg, ~1 × 10^{-5} mol) in the drybox and removed to the vacuum line on needle valve adapters. The NMR tube was degassed, and after transfer of deuterated solvent, the volatile reagents were introduced by vacuum transfer via calibrated gas bulb at −196 °C. The tubes were then sealed with a torch. Solid substrates were loaded with the metal complex, followed by solvent transfer on the vacuum line and flame sealing.

16. (^{t}Bu$_3$SiN)$_2$(^{t}Bu$_3$SiNH)WH (2) + Excess Oxirane. Compound **2** and 5 equiv of C_2H_4O were allowed to react at 23 °C for 5 days. The ^{1}H and ^{13}C{^{1}H} NMR spectra indicated quantitative formation of (^{t}Bu$_3$SiN)$_2$(^{t}Bu$_3$SiNH)WOEt (**9**).

17. (^{t}Bu$_3$SiN)$_2$WHCl(py) (4-py) + DME. 4-py and 33 equiv of DME were allowed to react at 125 °C for 23 h in C_6D_6. ^{1}H NMR spectroscopy indicated the formation of (^{t}Bu$_3$SiN)$_2$WCl(OMe) (**7**) and EtOMe (δ 1.24 (t, CH_3), 3.25 (q, CH_2)), in addition to unidentified degradation products.

Single-Crystal X-ray Diffraction Studies. General CCD Procedure. An appropriately sized crystal was loaded in a glass capillary tube and sealed, immersed in polyisobutylene and extracted out with a glass fiber, or placed onto a diffraction loop,[36,37] and then it was placed on the goniometer head of a Siemens SMART CCD Area Detector system equipped with a fine-focus molybdenum X-ray tube (λ=0.710 73 Å). Preliminary diffraction data revealed the crystal system. A hemisphere routine was used for data collection and determination of lattice constants. The space group was identified, and the data were processed with the Bruker SAINT program and corrected for absorption by SADABS. The structure was solved by direct methods (SHELXS), completed by subsequent difference Fourier syntheses, and refined by full-matrix least-squares procedures (SHELXL).

18. [(^{t}Bu$_3$SiN)$_2$WCl]$_2$ (1). A red crystal (0.2 mm × 0.2 mm × 0.1 mm) of **1** was obtained by slow evaporation of a saturated hexane solution. A set of 23 390 reflections were collected, of which 7281 were symmetry independent (R_{int} = 0.1404). The diffraction pattern showed reflections from a second crystallite which rendered data processing difficult. Constraints were applied to the geometries of the ^{t}Bu$_3$Si fragments on each ^{t}Bu$_3$SiNH ligand such that chemically equivalent inter- and intra-atomic distances were constrained to equal the same least-squares variables (e.g., all d(SiC_q) are equivalent, all d(C_qC) are equivalent, etc.). The core W, N, and Si atoms were refined with anisotropic displacement parameters, whereas all carbon atoms were refined isotropically because of the limited data set. All hydrogen atoms were included at calculated positions.

19. (^{t}Bu$_3$SiN)$_2$(^{t}Bu$_3$SiNH)WH (2). A colorless crystal (0.6 mm × 0.3 mm × 0.2 mm) of **2** was obtained by slow evaporation of a saturated diethyl ether solution at −23 °C. A set of 25 801 reflections were collected, of which 9840 were symmetry independent (R_{int} = 0.0358). After an initial refinement with all non-hydrogen atoms treated anisotropically, the difference Fourier map exhibited a maximum with reasonable geometric parameters for a terminal hydride. This atom underwent successful isotropic refinement. All non-hydrogen atoms were refined with anisotropic displacement parameters, and organic hydrogen atoms were included at calculated positions. The imide and amide groups were statistically disordered, as described in the text.

20. (^{t}Bu$_3$SiN)$_2$HW(μ-Cl)(μ-H)$_2$W(NSi^{t}Bu$_3$)py$_2$ (5-py$_2$). A dark purple crystal (0.3 mm × 0.2 mm × 0.5 mm) of **5**-py$_2$ was obtained by slow evaporation of a saturated pentane solution. A set of 26 495 reflections were collected, of which 7341 were symmetry independent (R_{int} = 0.0790). After an initial refinement, all non-hydrogen atoms were treated and refined anisotropically, and the difference Fourier map exhibited maxima consistent with two asymmetrically bridging hydrides; the terminal hydride was fixed.

21. (^{t}Bu$_3$SiN)$_2$WCl$_2$(py) (6-py). A colorless crystal (0.1 mm × 0.05 mm × 0.05 mm) of **6**-py was obtained by slow evaporation of a saturated pentane solution. A set of 11 393 reflections were collected, of which 3020 were symmetry independent (R_{int} = 0.0616). After an initial refinement, all non-hydrogen atoms were treated and refined anisotropically.

22. (^{t}Bu$_3$SiNH)(^{t}Bu$_3$SiN)WCl(PhCCPh) (12). An amber crystal (0.4 mm × 0.1 mm × 0.1 mm) of **12** was obtained by slow evaporation of a saturated benzene solution. A set of 44 227 reflections were collected, of which 10 173 were symmetry independent (R_{int} = 0.0720). After an initial refinement, all non-hydrogen atoms were treated and refined anisotropically.

CHESS Data Collection. 23. (^{t}Bu$_3$SiN)$_2$WCl(*trans*-CPh=CPhH) (11-*trans*). An amber crystal (0.4 mm × 0.1 mm × 0.1 mm) of **11**-*trans*, obtained by slow evaporation of a saturated THF/MeCN solution, was immersed in polyisobutylene and placed onto a diffraction loop.[36,37] All data were collected at the Cornell High Energy Synchrotron Source (CHESS). The X-ray wavelength was 0.943 Å, and the crystal-to-detector distance was set at 80 mm. A 2048 × 2048 pixel array CCD detector was employed, and data were collected as 10 s, 10°

(36) A throrough explanation of the construction of fiber loops and experimental methods at CHESS is given in: Walter, R. L. Ph.D. Thesis, Cornell University, Ithaca, NY, 1996.

(37) (a) Thiel, D. J.; Walter, R. L.; Ealick, S. E.; Bilderback, D. H.; Tate, M. W.; Gruner, S. M.; Eikenberry, E. F. *Rev. Sci. Instrum.* **1995**, *3*, 835−844. (b) Walter, R. L.; Thiel, D. J.; Barna, S. L.; Tate, M. W.; Wall, M. E.; Eikenberry, E. F.; Gruner, S. M.; Ealick, S. E. *Structure* **1995**, *3*, 835−844.

rotations, with the total rotation = 360°. All data were indexed and scaled using DENZO[38] and SCALEPACK programs, respectively. The space group was determined to be $P2_1/c$, and 5625 reflections, 3393 of which were symmetry independent ($R_{int} = 0.0616$), were subsequently processed with the Bruker SAINT program. Absorption corrections were performed using the SADABS program, and the structure was solved by direct methods (SHELXS), completed by subsequent difference Fourier syntheses, and refined by full-matrix least-squares procedures (SHELXL). After an initial refinement, all non-hydrogen atoms were treated and refined anisotropically.

(38) Otwinski, Z. *DENZO, a Program for Automatic Evaluation of Film Densities*; Department for Molecular Biophysics and Biochemistry, Yale University: New Haven, CT, 1988.

Acknowledgment. We thank the National Science Foundation (Grant CHE-9528914) and Cornell University for support of this research.

Supporting Information Available: CIF files pertaining to [(^{t}Bu$_3$SiN)$_2$WCl]$_2$ (**1**), (^{t}Bu$_3$SiN)$_2$(^{t}Bu$_3$SiNH)WH (**2**), (^{t}Bu$_3$SiN)$_2$HW(μ-Cl)(μ-H)$_2$W(NSi^{t}Bu$_3$)py$_2$ (**5**-py$_2$), (^{t}Bu$_3$SiN)$_2$WCl$_2$(py) (**6**-py), (^{t}Bu$_3$SiN)$_2$WCl(*trans*-CPh=CPhH) (**11**-*trans*), and (^{t}Bu$_3$SiNH)(^{t}Bu$_3$SiN)WCl(PhCCPh) (**12**); IR spectra and detailed X-ray crystallographic experimental descriptions (PDF). This material is available free of charge via the Internet at http://pubs.acs.org.

JA010957H